INTERMITTENT WATER DISTRIBUTION SYSTEMS: MONITORING, MODELLING AND IMPROVING EQUITY AMONG USERS

1. Introduction

1.1. Research problem statement

Water Distribution Systems (WDSs) are complex infrastructures designed to process, store and supply potable water to consumers continuously and reliably. However, hundreds of millions people around the world (both in developing countries and in developed ones) receive water intermittently. The intermittency in water supply is never a design choice: a common scenario is that the WDS initially provides water continuously but its ability to satisfy the users' demand is later limited by unpredicted changes (Kumpel and Nelson, 2015). Under intermittent conditions, WDSs can supply water for periods less than 7 days a week and/or for less than 24 hours a day. Alternatively, they can supply water for the whole 24 hours but making only a fraction of the water daily demand available. In both cases, the WDS behaves as an intermittent system, with network end users that may have access to water in a discontinuous way.

Despite water resource scarcity is often put forward by water service companies as the primary explanation for intermittent operation, environmental constraints constitute only one aspect of a multi-dimensional problem. Overemphasis on natural resource constraints risks under-valuing the human drivers that often reinforce intermittent supply. Moreover, the analysis of the causal-consequential pathways of such systems highlights that intermittency

in water supply has consequences that reinforce its causes in a sort of complex negative feedback loop (Galaitsi *et al.*, 2016).

The conversion of WDSs from intermittent to continuous supply is not obvious at all. In developed countries, water supply intermittency may be caused by temporal events such as droughts, pollution accidents, earthquakes, and maintenance operations. In such cases water supply usually normalises when the causal factors are over. Instead, in many developing countries, the intermittency in water supply is the common and rooted way of operation. Finally, sometimes intermittent WDSs are mandatory both in developed and developing countries because there are not the conditions for switching to continuous supply (infrastructure problems, severe water scarcity).

In comparison with continuous WDSs, intermittent ones are less studied despite of the size of population affected by this supply management. The available literature on the topic mostly focuses on the analysis of causes and consequences of intermittent WDSs at a macro-scale. Very few studies concern the hydraulic behaviour of such complex systems. Experimental data on intermittent WDSs are rather scarce. Moreover, traditional software tools for the modelling of continuous WDSs are not suitable for the simulation of water distribution networks subject to intermittency. As a consequence of all the above, there is a gap in knowledge concerning the behaviour of intermittent WDSs. This gap also prevents the planning of

design/managing strategies aimed at mitigating the negative impacts of intermittency in water supply.

1.2. Research goals

The aim of this research is to make a step forward in the analysis of intermittent WDSs both from experimental and modelling side. In particular, the first objective is to select a proper software tool for the modelling of intermittent WDSs, based on a preliminary theoretical study of the hydraulic behaviour of such systems. In order to test the ability of the selected software to correctly reproduce complex phenomena occurring in intermittent WDSs, experimental data on real intermittent water networks have been collected to validate the simulation results. The comparison with another model traditionally used in literature for the analysis of intermittent WDSs has been also useful to define the range of applicability of the selected software. Once the software has been set-up and validated, inequity in water resource distribution among network users of intermittent WDSs is analysed. The second objective of the research is the proposal of relatively simple and cheap operational/managing strategies aimed at improving (in the short term) the level of equity in existing intermittent WDSs. In particular, the effect on equity of changing the water circulation inside the network through the installation of control valves in specific pipes is investigated. Optimization algorithms have been set-up with the aim of finding valves locations

and settings to achieve the objective of an improved allocation of the water resource among the network users.

1.3. Thesis overview

The present thesis is organized as explained in this section. After the introduction to the topic (chapter 1), a summary of the literature state-of-the-art about intermittent WDSs is reported (chapter 2). In the core of the thesis the research methodologies (chapter 3), the case studies used to test the methodologies and the obtained results (chapter 4) are presented. Chapter 4 is divided in 3 main sections. Each section is dedicated to a specific case study. The thesis ends with a chapter of conclusions in which future perspective of the research are discussed. The supplementary material and the list of references are available in the end pages of the manuscript.

2. Background on intermittent WDSs

2.1. Causes and impacts

First part of the literature review on the research topic has involved the analysis of causes and impacts of intermittent WDSs, with a focus on the issue of inequity in water distribution among users. Current approaches in the modelling of intermittent WDSs have been analysed with the objective to identify a valid simulation tool for all the development of the analysis in the successive stages of the research.

Causes of intermittency in water supply are so many and so interconnected that isolating a more specific one is difficult (Simukonda *et al.*, 2018). Many authors agree in identifying the primary reason for intermittency in water supply in the scarcity of the water resource. However, a distinction should be made between absolute scarcity of water and scarcity due to economic or technical reasons, as Klingel (2012) proposes. Absolute scarcity means that water resources are insufficient to fully satisfy demand. If developing new water resources or curbing consumption by demand management methods are not possible options, absolute scarcity is a boundary condition that cannot be changed. Instead, in cases of technical-economic scarcity of water, the available water resources are in principle sufficient to cover the demand. Scarcity results from a reduction of the available water volume due to external factors such as water losses during distribution, wasting of water at the consumer end, poor electricity supply (essential for pumping stations), insufficiency of the water supply infrastructure itself, etc. In these cases, continuous water supply is still possible if all the technical-economic issues can be figured out. In their review on causal factors and problems related to intermittent WDSs, Simukonda *et al.*, (2018) highlight as demographic dynamics and hydrological regime changes can generate intermittency in water supply even in countries that did not suffer from water resource scarcity before. The rapid increase in population is even worsened by the simultaneous effects of urbanization, with high concentration of people in cities leading to

demands for water and sanitation services beyond the existing infrastructure capacity. Although this problem regards both developing and developed countries, the first ones suffer the most the consequences. In fact, as Klingel (2012) notices, developing countries are more likely characterized by a lack of an overarching system concept that would allow to consider mutual interactions between all the components of the WDS (pipes, tanks, pumping stations, feeders, valves, etc) as well as to take into account future developments of the network in the design phase. Many of these WDSs were designed in part with a concept in mind and were then extended and modified without any underlying plan. As hydrological regime changes are concerned, they can be climate or land-use related. Increases in drought frequency and duration have been observed in many parts of the World (Commission of the European Communities 2007; European Commission 2012) with heavy and long-lasting effects on water supply. On the other hand, the progressive deforestation due to agriculture, settlements and timber harvesting increase non-point source water pollution, surface runoff, sediment loads and irrigation water demand in dry seasons.

Impacts of intermittency in water distribution are several and affect both water quantity and quality as well as the state of the water supply infrastructure itself. From a hydraulic point of view, intermittent water supply implies continuous and cyclical phases of network filling and emptying. Pipes alternatively switch from free-surface to pressurized flow conditions. Users try to collect water as

much as possible during the supply hours often storing additional water volumes into private tanks that work as backup source during no-supply hours. The extraction of relatively large water volumes in a relatively short time leads peak load factors to assume values for which most piping systems were not designed (Klingel, 2012; Simukonda *et al.*, 2018). This causes large head losses and, consequently, pressure deficits in the system. The network infrastructure is subject to a significant stress and become even more vulnerable as a result of pressure surges and fluctuations. The consequences are restricted functioning of systems elements, higher rates of pipe breaks and associated major losses of water that end to worsen the root problem of water scarcity. The problem is aggravated even further by the poor system knowledge characteristic of intermittent WDSs and in part justified by the impossibility to apply common measurement and detection techniques to such networks. In fact, the regular filling/emptying of network pipes can result in faulty flow measurements. Moreover, when the supply system is not permanently filled with water under pressure, usual techniques of leakages detection cannot be easily applied.

The hydraulic behaviour described above has also impacts on the water quality. Detention of water in system pipes and in users' private tanks may entail the hazard of colonization of water bacterial pathogens. Moreover, low systems pressure allows particles and ground water to enter the pipes through the weak points of the network. Consequences may be particularly severe where sewers

pipes run parallel to drinking water ones. Finally, intermittent WDSs progressively induce a hygiene behaviour deterioration. The reduction in water consumption and in frequency of washing, as well as the increase of water sharing among family members, induce additional health risks (Mokssit *et al.*, 2018).

Intermittent supply is often associated to a higher wastage of water as compared to continuous supply (Mokssit *et al.*, 2018; Simukonda *et al.*, 2018; Klingel, 2012). This paradoxical situation is a salient example of the interweaving between causes and consequences of intermittency. Wastage of water is mainly a consequence of the relatively large volume of water supplied in a short period of time. Underdesigned private tanks not controlled by float valves can overflow during the supply period. Moreover, a typical behaviour of consumers in high-pressure areas is to empty unused stocked volume of water each time the supply is restored in order to create capacity for fresh water. These wastage acts take place while consumers in low-pressure areas have little or no water at all.

2.2. Equity in water distribution among users

Besides all the technical impacts and consumers behaviour described above, the higher social cost of intermittent WDSs is the resulting inequity in water distribution among the network users. The scientific literature about equity in water distribution mostly regards irrigation water delivery systems that are traditionally designed to operate intermittently. In civil intermittent WDSs, the non-uniformity

in space and time in water allocation among users is directly associated to the non-uniformity in pressure distribution among the network nodes. This problem is even exacerbated in big networks characterized by high gradients in elevation because of the significant differences in nodal pressure throughout the system. Moreover, the topological structure of the network makes some points more advantaged than others because of their elevation or their proximity to the supply reservoir (Fontanazza *et al*., 2007; Ameyaw *et al*., 2013). As Mokssit (2018) highlights, each node is characterized by a different water reception time (i.e., the time needed for the node to receive the water from the beginning of the supply period), depending on its position on the network. For the most disadvantaged nodes, the reception time may be greater than the supply duration. The situation is even worsened by the progressive installation of private tanks (i.e., roof or basement tanks) at the end users (Arregui *et al*., 2006; Cobacho *et al*., 2008; Criminisi *et al*., 2009). Private tanks offer significant advantages for the users; importantly, they can store water during supply hours as back-up source for non-supply hours. However, installation of private tanks exacerbates problems of intermittent WDSs as it introduces complexity to the network and increases the risk of additional inequity in water distribution. In fact, filling the tanks causes peaks flows to increase, which, in turn, generate significant head losses thus amplifying the pressure differences between the collection points in the network (Mokssit, 2018; Fontanazza *et al*., 2007). De Marchis *et al*. (2011) have analysed the

spatial and temporal non-homogeneity of the water distribution among users in a WDS in southern Italy in presence of private tanks at the household scale. The authors remarked that private tanks always increase water distribution inequity, even when the available water resource is sufficient to cover the full demand. As a result, some users get more water than others, thus achieving a higher level of satisfaction of their water demand.

First issue in studies about equity in WDSs concerns the definition of a measure of the equity itself. Though the concept of equity seems very simple, it could be useful to distinguish between "absolute" and "relative" equity. In fact, being the access to water a fundamental human need, equity can be defined (with a focus on the single user) as the delivery of a fair share of water to consumers (Molden and Gates, 1990). However, the "fair share" is often interpreted subjectively. Moreover, since users are part of a system, the concept of equity should be also evaluated in comparative terms (how much water users are getting in comparison to other users?). According to this interpretation, in a WDS, equity issues should involve an equal level of satisfaction of all the network users.

Different ways to measure equity have been proposed in literature. Fontanazza *et al*. (2007) used the following performance indices to evaluate equity in distribution during intermittent operational conditions:

$$EQ1=\frac{V_{int}}{V_{cont}}$$

$$EQ2=\frac{Q_{int,t}}{Q_{cont,t}} \quad (1)$$

where V_{int} is the water volume supplied to users in a service cycle, V_{cont} is the requested user water volume in the same period, $Q_{int,t}$ and $Q_{cont,t}$ are the average water flows supplied to users at time t in intermittent and continuous distribution conditions, respectively. A service cycle is the time lag between two subsequent activations of water service in intermittent distribution conditions. Basically, if *EQ2* is evaluated at time t equal to the end of a service cycle, its value coincides with that of *EQ1*. Indices in Eq. (1) are evaluated for all the network nodes and range from 0 to 1. The first index allows to identify the users that obtain less water than their needs ($EQ1<1$) and the advantaged users that get water volumes equal or even higher than their needs ($EQ1\geq1$). But even if globally in a service cycle water volume distributed at the users do not greatly differs among them, wide differences may be possible during the distribution period because advantaged users can fill their reservoirs much faster than disadvantaged ones. This aspect can modify the users' perception of the water service reliability. For this reason, the index *EQ2* can be useful for analysing the behaviour of the network in different moment of the service period and analysis eventual temporal disparities among nodes. An evaluation of the inequalities among the network users can derive from the comparison of values of the two indices for

the different nodes. However, the authors have not used a single global system parameter to evaluate inequity in the WDS.

De Marchis *et al*. (2011) proposed the following synthetic indicators to explain inequalities in WDSs under different water shortage scenarios:

$$WV_t^j = \frac{\int_0^t Q_{up}^j(t)\mathrm{d}t}{\int_0^{24} D^j(t)\mathrm{d}t}$$

$$WV_{global,t} = \sum_{j=1}^{N} WV_t^j \, p^j \qquad (2)$$

where $Q_{up}^j(t)$ is the flow supplied to node j at time t, $D^j(t)$ is the corresponding water demand (for the same node and at the same time) and p_j is the weight the j-th node, calculated as the ratio between the daily water demand of the users connected to the j-th node and the users daily water demand of the whole network. The first indicator is calculated for all the N network nodes and expresses the ratio between water volumes supplied over time and daily water demand of the users connected to the j-th node. In normal condition of supply, it grows progressively during the day following the users' water demand and it is equal to 1 at the end of the day. In water scarcity conditions, it is always lower than 1 for all those disadvantaged users that are not able to satisfy their water demand. The second indicator instead is a weighted average ranging from 0 to 1 and used as global system parameter. At the end of the day $WV_{global,t}$ is equal to the ratio of the water volume supplied to the network and the total water

volume requested by the network. Therefore, the maximum value of the global indicator depends on the water shortage scenario analysed. In a water shortage scenario $WV_{global,t}$ cannot be equal to 1, even in case of equal level of satisfaction of all the network users.

More recently, Gottipati *et al*. (2014) proposed a single uniformity coefficient *UC* to evaluate the global equity in water distribution among the network users at the daily scale:

$$UC=1-\frac{ADEV}{ASR} \tag{3}$$

where $ASR=\sum SR/N$ is the daily average of the supply ratios *SR* of all the *N* network demand nodes (nodal *SR* provided by the ratio of the supplied water volume to the demand volume), and $ADEV=\sum|SR-ASR|/N$ is the daily average of absolute deviations from *ASR* of the supply ratios of all the *N* demand nodes in the WDS. Coefficient *UC* provides a comprehensive index for the evaluation of the equity in water distribution among the nodes of the WDS during the day. It is based on the concept that maximizing the equity in the network is equivalent to minimizing the variations among users (Ameyaw *et al*., 2013). Eq. (3) shows that values of $UC<1$ indicate non-uniformity in the distribution among users, while $UC=1$ represents conditions of maximum equity (i.e., all users have the same level of satisfaction). Condition $UC=1$ can be obtained even in scenarios of water shortage if all network nodes perform with the same value of $SR<1$. As an example, let us consider a WDS subject to rationing conditions that

determine a value of supply equal to 70% of the total network water demand. If all the nodes of the WDS receive the same level of service, their supply ratio is the same (and equal to SR=0.7), thus providing $ADEV$=0 and UC=1 (according to Eq. 1). Under the same hypothesis, the global coefficient $WV_{global,t}$ in Eq. (2) would be equal to 0.7. The maximum value of SR that can be achieved by all nodes in a specific water shortage scenario and in condition of maximum equity can be assumed as an "equity threshold" (ET) for the users of the network. Nodes with $SR>ET$, are advantaged as they get more water than they should; conversely, nodes with $SR<ET$ are disadvantaged as they get less water than the equity threshold. Thanks to its simplicity and its ability to summarize the level of equity of the whole network regardless of the water shortage scenario, the index described by Eq. (3) was chosen to evaluate the global equity in WDSs in all the elaborations presented in this thesis.

In the last decade, some authors investigated strategies to improve equity in water distribution among the network users. Ameyaw *et al.*, (2013) have used a multi-objective optimisation model to maximize equity and minimize the cost in intermittent WDSs by varying the size and the location of users' private tanks. The model was applied to a simple example network showing that the best equity level is associated with the highest total cost and vice versa. A balance must be made between consumer concerns on equity and the water utility's financial strength. Gottipati and Nanduri (2014) have shown the equity in water distribution to be affected by several factors. The

results of their study, based on EPANET simulations, can be summarized as follows:

- equity in WDSs is affected by the water level inside the supply reservoir;
- equity in water distribution is also affected by the variation of demands at certain nodes. For example, by making demand 0 at certain nodes that are very close to or very far off from the reservoir, equity can be improved considerably. Therefore, planning staggered supply hours within the network may be considered as an effective measure to improve the equity in distribution;
- diameter of pipes, position in the network of the supply reservoir and the layout of the network itself greatly affect the distribution of the water resource among users.

Ilaya-Ayza *et al*. (2017a) have performed a multi-criteria optimization of supply schedule in intermittent WDNs taking into account equity issues. In this regard, the possibility to organize the network in sectors (also called district-metered areas) would be very useful since supply schedules can be more easily established (Ilaya-Ayza *et al*., 2017b). However, most of these methods require implementation of radical modifications in the network layout incurring large capital costs. Therefore, their practical application may be afforded only with reference to the planning/design or in the long-term upgrade stages of WDSs. Conversely, studies concerning setup of operational strategies (at low cost of implementation) for improving water

distribution equity in existing WDSs are rather limited. Moreover, the suitability of the software/tools for the simulation of intermittent WDSs used in the cited studies about equity has not been verified, yet.

2.3. Current approaches in modelling

The possibility to study the effects of operational strategies aimed at mitigating the several negative impacts of intermittent WDSs requests the use of a proper simulation tool. Traditional software/tools for WDSs such as EPANET (Rossman 2000) do not allow for simulating transient flows, thus being unable to analyse intermittent supply in a proper way. Moreover, the demand-driven formulation traditionally used in the modelling of WDSs is not suitable for network subject to water intermittency. In fact, due to pressure deficit, demand in intermittent WDSs is better described using a pressure-driven formulation. The network filling phase is the most complex and currently least studied phase of intermittent WDSs. Available experimental data regarding processes during the network filling are rather scarce (De Marchis *et al*. 2010). Earlier studies on the pipes process of intermittent WDSs were carried out by Liou and Hunt (1996). The authors developed a numerical model to describe the unsteady motion of a lengthening rigid water column (RWC) filling an empty pipeline with an undulating elevation profile. The model is applicable when the discharge velocity is sufficiently high or when the pipe diameter is sufficiently small so that air intrusion does not occur. Improvements of this model were proposed by De Marchis *et al*. (2010) and applied with success to a portion of the water distribution

network of the city of Palermo, in Italy. In particular, the authors removed the hypothesis of fluid incompressibility (RWC theory) which can be accepted for simple pipeline systems but may be not sufficient for complex water distribution networks. Cabrera-Bejar and Tzatchkov (2009) firstly hypothesized the use of the software EPA-SWMM (Rossman 2015) – developed for the analysis of urban drainage systems – for the simulation of the initial filling process of intermittent WDSs. The authors first explored the possibility to use particular settings of the software to correctly model water distribution networks. Although advantages of using this freeware software have been highlighted by the authors, results have not been validated yet by field experiments or compared to previous modelling results from the literature.

3. Methodologies

3.1. Hydraulic behaviour

Intermittent WDSs are cyclically subject to three main phases: 1) the initial network filling at the beginning of the water supply period, 2) a phase of functioning under pressure conditions and, finally, 3) the network emptying when the supply period is over. The duration of each of these phases depends on both the water supply management criteria and the network characteristics. For large districts with short duration of the supply period, the network functioning under pressure conditions may be very short. During the filling process, the network pipelines are progressively filled with

water. Complex phenomena of unsteady flow with significant variation in flow velocity and water head occur in the network during this process. Each pipe of the network can be in one of the following conditions: i) the pipe is empty, ii) the pipe is being filled at one end side, iii) the pipe is being filled at both ends, and iv) the pipe is already full. In particular, condition iii) is typical of looped or multi-source networks. Moreover, the filling process can evolve in different ways based on the network characteristics and on the supply modalities from the source. If the flow covers the pipe cross section partially, free-surface flow occurs with (ideally) atmospheric pressure at the water-air interface. In that case, the pipe filling may proceed as a backwater process, with the downstream pipes of the network being filled first. Conversely, if the water flow covers the full cross section, pressure flow occurs during the filling process. In this second case, the filling process normally proceeds forward from upstream to downstream pipes and the farthest conduits from the upstream source are the last to be filled. In addition, the flow variability leads to switch from pressure to free-surface flow condition in the network. For instance, during the filling process, pressure and free-surface flow conditions may coexist in different portions of the network because of differences in pressure due to head losses. Evidently, the modality of the network filling has a profound impact on the system spatial/temporal water distribution, thus determining which users may access to water first and which have to wait for longer time. Moreover, due to additional

capacities represented by private tanks, more time might be required to complete the network filling process.

Later, if the supply duration is greater than the network filling time, the WDS experiences the phase 2 of functioning under pressure condition. However, during this phase private tanks continue to be filled with water so that pressures in the network are generally lower than those typical of continuous WDSs. In fact, the refilling of the tanks is usually controlled by float valves, so that the inflow to the tanks does not stop unless they are totally full.

Finally, when the supply period is over, the network emptying (phase 3) completes the cycle of intermittent WDSs. Starting from this moment and until the beginning of the next supply period, users' needs can be satisfied exclusively by back-up water collected inside the private tanks. In some cases, the perception of the risk of limited access to water for long time may lead users to install oversized tanks, that sharpen the consequences of intermittency.

The cyclic phases described above are typically defined for those systems that opt for suppling water for period less than 24 hours per day and/or less than 7 days per week. As reported in the introduction, another way to manage water shortage scenarios is to supply a fraction of the water demand continuously for the 24 hours a day (Ameyaw *et al.*, 2013, Soltanjalili *et al.*, 2013). In this case may be very difficult to distinguish clearly the occurrence of different phases. The network is generally in conditions of pressure deficit both because

it is supplied with an amount of water smaller than the demand value and because of the presence of private tanks. Pipes can switch from free-surface to pressurized flow according to the network demand (which depends on both the time of the day and the current water level inside private tanks). Therefore, the network behaviour (from a hydraulic point of view) is very close to the case of water supplied intermittently from the source.

Previous analysis is more the result of theoretical studies and field experience about intermittency rather than of experimental observations. As discussed in the introduction, experimental data about intermittent WDSs are scarce. As a consequence, the few proposed approaches to model such systems have not been usually validated through comparison with data available from the field.

3.2. Used models for intermittent WDSs

Following the research goals, the first objective of the project is to evaluate the potential of EPA-SWMM software in the simulation of intermittent WDSs. To achieve this objective, tools available in EPA-SWMM software were adapted in a novel way for the modelling of components and operational modalities of intermittent WDS. The results provided by the software were validated trough comparison with both experimental observations and results provided by a model based on the theory of the RWC (traditionally used for the simulation of the filling phase of intermittent WDSs). All the settings in EPA-

SWMM software needed for the modelling of intermittent WDSs and the RWC model are described in the following sub-sections.

3.2.1. EPA-SWMM software

The Storm Water Management Model (SWMM) is a free and open-source software developed by the United State Environmental Protection Agency (USEPA) with the original objective to simulate flows in urban drainage systems. Thanks to its availability (freeware) and its simple and intuitive user interface, EPA-SWMM is widely used for hydraulic simulations of urban drainage systems.

The last available release of the software (version 5.1) was used in this work (Rossman, 2015). The routing portion of EPA-SWMM allows describing runoff flow propagation through a system of conduits, channels, storage facilities, as well as devices such as pumps and other regulators. Unsteady flow propagation in EPA-SWMM is modelled through the De Saint Venant (DSV) partial differential equations for the conservation of mass and flow momentum:

$$\frac{\partial A}{\partial t}+\frac{\partial Q}{\partial x}=0$$
$$\frac{\partial Q}{\partial t}+\frac{\partial (Q^2/A)}{\partial x}+gA\frac{\partial H}{\partial x}+gAS_f=0 \qquad (4)$$

Simultaneous solution of DSV equations for each conduit, coupled with the continuity equation:

$$\frac{\partial H}{\partial t}=\frac{\sum Q}{A_S} \qquad (5)$$

at each network node provides information on the spatial and temporal variation of water levels and flow discharges throughout the network. In Eqs. (4) and (5), x and t are the spatial and temporal variables, respectively, A [m^2] is the wetted area of the flow in the pipe cross section, Q [m^3/s] is the flow in the pipe, H [m] is the nodal piezometric head (sum of geodetic elevation and water level), $\sum Q$ [m^3/s] is the net inflow to the node (inflow–outflow). A_S [m^2] is defined as the "node assembly" surface area and is calculated based on the horizontal surface area of both the node (when available) and half the length of each conduit linked to the node itself (Rossman, 2015).

EPA-SWMM can be applied to any network layout, even those containing multiple downstream diversions and loops. This can be obtained by running the model using the dynamic wave analysis option that allows also to model channel storage, pipe backwater effects, and pressurized flow.

In principle, although the software was originally conceived for the simulation of urban drainage systems, its capability to simulate the transition from free-surface to pressurized flow makes it suitable also for the simulation of intermittent WDS. However, a customized use of EPA-SWMM tools and utilities is required for the correct description of processes occurring during intermittent water supply. As suggested in early studies by Cabrera-Bejar and Tzatchkov (2009) and Shrestha and Buchberger (2012) the following software

modes/settings should be adopted for the simulation of intermittent WDSs:

- supply tanks/reservoirs showing variation in water level could be modelled as storage nodes by proper definition of the tank size. An inflow pattern to the tank is provided as input to the model through the storage node property;
- very large values of surcharge depth (hundred meters) have to be prescribed at network junctions to exclude overflow from nodes (as flooding) during pressurized condition.

Previous assumptions are not sufficient for reliable and accurate simulations. Therefore, additional settings and tools of EPA-SWMM were adopted in a novel way in the research work presented in this thesis to correctly describe the operation of intermittent WDSs:

- supply tanks/reservoirs with constant water level were modelled using the storage node tool for which large values of the bottom area are assumed, thus neglecting water level variations during the supply;
- a negligible value of the minimum nodal surface area was assigned to all network nodes (this parameter is used by EPA-SWMM to compute the nodal piezometric head in Eq. (4) when A_s is less than the minimum nodal surface area defined by the user);
- specific control rules for pipes connected to the supply reservoir were implemented to simulate the instantaneous opening of a gate valve at the beginning of the supply period;

- flow supplied to the users at each demand node was modelled using available elements of the software such as outlet links and outfall nodes in a customized way. In particular, a rating curve was associated to the outlet link of each demand node to describe the pressure-driven function proposed by Wagner *et al*. (1988):

$$\begin{aligned} Q_{user} &= 0 && \text{for } p<p_{min} \\ Q_{user} &= Q_{req}\left(\frac{p-p_{min}}{p_{req}-p_{min}}\right)^{\beta} && \text{for } p_{min}<p<p_{req} \\ Q_{user} &= Q_{req} && \text{for } p>p_{req} \end{aligned} \qquad (6)$$

  where Q_{req} [m^3/s] is the required nodal demand, p [N/m^2] is the current pressure at the node, p_{min} [N/m^2] is the minimum pressure required to get flow from the node, p_{req} [N/m^2] is the pressure required for the full satisfaction of users demand at the node and β is a calibration parameter typically ranging from 0.5 to 1 (Fontanazza *et al*., 2007; Campisano and Modica, 2016; Braun *et al*., 2017; Ciaponi and Creaco, 2018);
- diurnal variations of nodal demands were prescribed through control rules, by adopting multipliers for the implemented rating curves;
- private tanks were modelled by using available tools of EPA-SWMM in a customized way. In particular, storage node elements with suitable size were used to model tanks, while the connection between the network node and the tank was simulated through outlet link elements. Among the relationships proposed in the literature to estimate the inflow to private tanks controlled by float

valves, the hyperbolic law of the emitter suggested by De Marchis *et al.*, 2015 was chosen for the simulations. The float valve emitter law was modified in order to include water losses occurring between the water network and the private tank. In this way, the formulation led to flow values consistent with those typical of domestic taps used to fill the tanks. Therefore, the filling cycle of private tanks is described by the following equations:

$$\begin{cases} Q=Q_{max}=C_v a_v \sqrt{2g[(h-z_t)-JL]} & H<H_{min} \\ Q=Q_{max}\tanh(mr)\tanh(nr) & H_{min}<H<H_{max} \\ Q=0 & H>H_{max} \end{cases} \quad (7)$$

where Q (m^3/s) is the inflow to the tank, Q_{max} (m^3/s) is the value of inflow when the float valve in fully open, C_v (-) is the float valve emitter coefficient, a_v (m^2) is the valve inflow area, g (m/s^2) is the value of gravity acceleration, h (m) is the piezometric head on the network connection node, z_t (m) is the elevation of the float valve, J (-) is the energy line slope, L (m) is the length of the pipe connection between the network and the tank, m and n are no-dimensional coefficients and r is the ratio $(H_{max}-H)/(H_{max}-H_{min})$, being H (m) the water level inside the tank, H_{max} (m) the value of water level in the tank that leads to a full closure of the valve and H_{min} (m) the value of water level in the tank under which the valve is fully open. The progressive closure of the orifice by the floating valve (for values of H between H_{min} and H_{max}) is obtained through

the use of control rules in EPA-SWMM, by prescribing reduction coefficients to Q_{max} with a fixed spatial step within the float valve excursion.

- available tools and settings of EPA-SWMM were used also to model valves. Fully closed valves (e.g., gate valves) were modelled by setting as "closed" the status of the conduits in which they are assumed to be placed (by use of the control rules editor of the software). Instead, simulation of control valves with different closure degree was carried out by adoption of an entry loss coefficient K (-) for conduits in which the valves are installed. Therefore, the head loss ΔH (m) provided by the device is evaluated by the model as:

$$\Delta H = K\frac{V^2}{2g} \tag{8}$$

being V (m/s) the flow velocity. Normally, K-values are provided by the manufacturer as a function of the valve degree of closure.

- water leakages were modelled by combining outlet links and outfall nodes, and by linking them to network nodes. Default function for outlet links was used to describe the power law discharge-pressure relationship commonly adopted in literature for water leakages (Thornton and Lambert 2005):

$$Q_p = ah^{\gamma} \tag{9}$$

being Q_p (m^3/s) the discharge due to leakages, h (m, water column) the nodal pressure head, a ($m^{3-\gamma}/s$) the leakage coefficient and γ the leakage exponent.

The spatial and temporal derivatives in Eqs. (4) and (5) are solved in EPA-SWMM for each time step, using the Eulerian finite differences method. The value of the simulation spatial step Δx was fixed as a compromise between the required computational effort and the desired accuracy of the output results. Then, the value of Δt was obtained according to the Courant–Friedrichs–Lewy (CFL) condition for the stability of the numerical scheme:

$$C=\frac{a\Delta t}{\Delta x}\leq 1 \tag{10}$$

where C is the Courant number and a [m/s] is the absolute celerity of the wave front during the filling process. The value of a varies step by step during the whole process and, at the same step, it is different pipe by pipe of the network. However, the maximum value of the flow velocity is generally achieved at the beginning of the filling phase, in correspondence of the tank outlet pipe (Liou and Hunt, 1996). In that case, the maximum value of a can be evaluated as:

$$a=V+c=\sqrt{2gH_t}+\sqrt{gh} \tag{11}$$

where c [m/s] is the relative wave celerity, H_t [m] is the tank piezometric head and h [m] is the water level in the tank outlet pipe. In safe conditions, the value of h was assumed equal to the diameter

of the pipe. Value of Δt as obtained from Eq. (10), with a evaluated according to Eq. (11) (safe condition), is then assumed as the routing time step in the settings of the simulation in the software.

3.2.2. RWC model

The RWC model - used for comparison of the simulation results obtained by EPA-SWMM - is based on the following assumptions (Liou and Hunt, 1996):

- the wave front of the water column always coincides with the pipe cross section;
- the pressure at the front is atmospheric;
- the water-pipe system is incompressible (i.e., the water column is rigid).

The first assumption would limit model applicability only to pipes conveying flow under pressure condition. Intuitively, this condition is verified for high flow rates in pipes characterized by relatively mild slope and small diameter. From a more rigorous theoretical point of view, such condition is achieved for those cases in which the flow velocity is larger than the celerity of air intruding the water column (Liou and Hunt, 1996). However, experiments by Guizani *et al*. (2005) disagree with these results and demonstrated that non-vertical wave fronts may develop even in these cases. The second assumption is commonly verified in WDS characterized by a relative high number of air entry/release valves through which air can entry or exit the system. The last assumption is usually adopted to simplify the

analytical description of the system but it may lead to unphysical values of pressure when the water column achieves a terminal pipe of the network or at those sections where two travelling water columns impact each other.

Under the previous assumptions and neglecting the kinetic head of the flow (Mays, 1999), the energy conservation equation applied to the rigid water column provides:

$$\frac{\partial}{\partial x}\left(z+\frac{p}{\gamma}\right)+\frac{1}{g}\frac{\partial V}{\partial t}+S_f=0 \tag{12}$$

where z [m] is the elevation of the network nodes, p/γ [m] is the piezometric height with p [N/m^2] the pressure at node and γ [N/m3] the water specific weight, g [m/s^2] is the gravity acceleration, S_f [-] is the energy line slope which can be estimated according to the Darcy-Weisbach equation (Darcy, 1857).

Equation (12) is solved twice for those pipes for which the filling process proceeds from both pipe ends simultaneously. For the time steps during which the two oppositely advancing columns meet one each other, the condition $\partial V/\partial t=0$ is prescribed in Eq. (12). The same condition is used when the water column reaches the downstream end of terminal pipes.

The mass continuity equation for each demand node:

$$\sum VA+Q_{user}=0 \tag{13}$$

is coupled to Eq. (12), being A [m²] the area of the pipe cross section (corresponding to the wetted area of the flow because of the hypothesis of the model), and Q_{user} [m³/s] the flow supplied at the demand node. Specifically, the pressure-driven function in (6) is used in the model demand node.

For nodes representing tanks/reservoirs, the mass continuity equation:

$$\frac{\partial h_s}{\partial t} = \frac{Q_{in} - \sum VA}{A_t} \tag{14}$$

is used in the model, where h_s [m] is the water level in the tank, Q_{in} [m³/s] is the tank inflow and A_t [m²] is the free-surface area of the tank. The sum in Eq. (14) is extended to all the outlet pipes connected to the tank.

Equations (12) to (14) are simultaneously solved by the model for each time step, using the finite differences method (Eulerian method). The numerical solution proceeds by fixing the time step Δt of the simulation and by computing the hydraulic parameters of the water column of length Δx.

It worth to underline that RWC model in its original form was used for comparison of the simulation results provided by EPA-SWMM even though an improved version of the model was proposed later by some authors (see section 2.3 of the background chapter). In the modified version of the model (De Marchis *et al*., 2010), the method

of characteristics was used to account for both water compressibility and pipeline deformability with a resulting more complex set of differential equations. However, the purpose of the research is to compare the filling process as simulated by EPA-SWMM with a model based on the assumption of only-pressure flow condition (hypothesis of vertical water front during the filling process both in the original RWC model and in the modified version). Therefore, the original e simple form of the RWC model was used for the comparison carried out in this work. Nevertheless, in future development of the research a comparison between EPA-SWMM and such improved numerical models for the network filling process could be implemented to find out the differences in model performance.

3.3. Control valves installation to improve equity

An operational strategy aimed at improving equity in WDSs under condition of water shortage was investigated. The strategy is based on the identification of optimal locations and settings of control valves in order to re-arrange the flow circulation in the network pipes and allow improved water distribution to end users. Two different methodologies were defined to find optimal valves location and setting. Firstly, the benefits in terms of improved equity in water distribution were evaluated using Sequential Addition (SA) algorithms. SA is based on the optimal location of each single valve one after the other, while maintaining in each step the optimal valves configuration already found in previous steps. Secondly, a multi-objectives genetic algorithm was adopted to analyse optimal position

and setting of valves. Genetic algorithms are randomized search algorithms that have been developed in an effort to imitate the mechanics of natural selection and genetics. In particular, the well-known Non-Dominated Sorted Genetic Algorithm II (NSGA II) (Deb *et al*., 2002) was used in this work. Although NSGA II has been widely adopted for optimization problems in continuous water distribution systems (Farmani *et al*., 2006; Alvisi & Franchini, 2009; Creaco *et al*., 2010, 2016; Creaco & Pezzinga 2018; Wang *et al*., 2019), there are no examples of application regarding intermittent WDNs.

EPA-SWMM software was used for the hydraulic simulation of the network in all the valves configurations. For each configuration, equity in water distribution was evaluated using index *UC* (Eq. 3). Preliminary studies on the network behaviour showed that intermittent systems are subject to a transitory phase (that may have a duration of several days from the initial condition) before achieving a condition of regime. Such transitory phase is due to the process of filling of the network that determines initial unbalance between input and output flows. The achievement of the condition of regime is verified when daily values of *SR* and *UC* do not change anymore during the simulation.

3.3.1. SA algorithms for optimal location of valves

The development of the SA algorithms proposed in this study moves from the early work by Pezzinga and Gueli (1999) concerning continuous water supply systems. Recently, SA was also used by

Creaco and Pezzinga (2018) for the identification of the optimal location of valves to reduce leakage in WDS. Two SA algorithms were set-up. The first SA algorithm assumes to install gate valves that modify the flow circulation in the network in order to maximize the global equity index. This objective is obtained irrespectively of the local impact of the new flow circulation on the level of supply satisfaction of each network node. Conversely, the second SA algorithm was developed with the aim of maximizing the global equity index by optimizing both location and settings of control valves, by taking into account also the effect of the new flow circulation on the supply at each node of the network. A detailed description of the two SA algorithms is reported below.

SA of gate valves

The rationale behind the adoption of this algorithm is to modify the flow circulation in the WDS by using gate valves with the aim of maximizing the daily value of *UC* at the condition of regime. The algorithm is based on the following steps:

1. a preliminary hydraulic simulation of the WDS without valves is carried out (no-valve scenario), and the daily value of *UC* is calculated using Eq. (3);
2. gate valves are placed in the network one at a time. A set of n_p (number of possible locations of gate valves in the network) simulations is carried out to search for the location of the first gate valve (valve 1) in the network that provides the largest daily value

of *UC*. The value of n_p usually coincides with the number of network pipes, unless particular pipes have to be excluded as possible location of gate valves;

3. n_p-1 simulations are carried out to search for the location of the second gate valve (valve 2) that provides the largest daily value of *UC* (being valve 1 already placed in the network according to step 2). In other words, all the pipes are evaluated as potential locations for valve 2, excluding the pipe selected for installing valve 1;
4. step 3 is repeated to maximize the value of *UC* until the benefits of adding a new gate valve (in terms of increase in *UC*) become negligible (increase smaller than 1%).

The described algorithm seeks to improve the global equity of the water distribution in the WDS. However, it does not take into account of eventual unfair decrease of single *SR* value (i.e., at the level of the single node) with respect to the no-valve scenario.

SA of control valves

The algorithm of SA of control valves aims at identifying valve locations and related closure settings in order to maximize the value of *UC* at regime, while respecting particular constraints on acceptable changes of single nodal *SR*. Acceptable values of *SR* are different for nodes starting with *SR*>*ET* or *SR*<*ET* in the no-valve scenario. Nodes with *SR*>*ET* (with an excess of supply as compared to the equity threshold) can decrease their *SR* down to *ET* in the configuration with valves installed. Instead, nodes with *SR*<*ET* are not allowed to further

reduce their value of *SR*. The operational steps to implement the algorithm are as follows:

1. the simulation of the network without valves installed is carried out as for step 1 of the procedure for the previous algorithm;
2. analogously to step 2 of the previous procedure, pipe-by-pipe simulations are carried out assuming control valve 1 to be located alternatively in one of the n_p possible locations in the network. The control valve in this step is assumed to be fully closed. Priority of location of the valves is identified according to the obtained values of *UC* (one for each simulation) that are sorted from the higher to the lower one;
3. the first location (i.e., the location in the list providing the maximum value of the daily *UC*) is firstly considered. Each node of the network is analysed to check if the placement of the valve does not result in unacceptable values of *SR* at each node of the network;
4. if the nodal check is not passed for one or more nodes of the network, targeted simulations are run to evaluate if closure settings with the same valve location can mitigate local negative impacts on single nodal *SR*. Operationally, the simulations are carried out with decreasing values of the valve loss coefficient *K* (Eq. 8) in order to consider the gradual increase in the opening of the valve until all the nodes of the network achieve acceptable values of *SR*. Conversely, if the check is still not satisfied for any of the settings of the valve, the first location in the list is discarded

and the procedure is repeated (starting from step 3) for the second location in the order of priority;

5. SA of control valve 2 is carried out by repeating the same steps, assuming valve 1 being already placed and set as for previous steps 3 and 4. Similarly to procedure discussed for the previous algorithm, all the pipes are evaluated as potential locations for valve 2, excluding the pipe identified for the installation of valve 1;
6. the procedure is terminated when SA of control valves does not provide further significant benefits in terms of *UC* (increase smaller than 1%).

3.3.2. NSGA II for optimal location of valves

NSGA II was adopted to find optimal location and setting of the valves in the WDS. This genetic algorithm (GA) uses two main modules - fast non-dominated sort and crowding distance – to evaluate the quality of solutions in the environmental selection. At each generation of NSGA-II, non-dominated sorting is first carried out to select solutions with lower ranks from the population, combining parent and offspring population. Then crowding distance is used as the secondary metric to distinguish solutions in the same rank by preferring those with a large crowding distance in order to promote diversity. Thanks to its speed, simplicity and effectiveness, NSGA II becomes the benchmark of the performance of other multi-objective optimization algorithms.

In the applications of the algorithm carried out in this work, integer values were used for individuals' genes. Generation, crossover and mutation procedures were adapted accordingly. The adaptive mutation operator described by Carvalho and Araujo (2009) was implemented in the GA. Individuals in the GA have a number of genes equal to n_p. Moreover, the number of population individuals and the total number of generations must be fixed in light of the trade-off between needed computational effort and accuracy of the results. An initial population was generated in the developed GA to properly address the first elaborations computed by the algorithm and to assure high computational efficiency of the optimization (Creaco and Pezzinga, 2018). In particular, the initial population contained individuals with only 1 valve, for all the possible valve locations, as well as the solution with 0 valves (no-valve scenario). In this way, the developed GA performs a complete initial exploration of the research space, assessing the most performant individuals to use as parents for successive iterations. It should be remarked that the initial population has a number of individuals equal to n_p. In case that the total number of population individuals is greater than n_p, the initial population is a portion of the population processed at first by the algorithm (the remaining individuals are generated randomly).

The various individuals of the GA are compared based on their fitness, which is determined according to two objective functions. The first objective function is the complement to unity of the uniformity coefficient in Eq. (3) (i.e., 1-*UC*), which is calculated through the

network simulation under the configuration of valves encoded in the algorithm for each individual solution. The second objective function is the number of valves (N_{val}) installed in the WDS, which is directly associated (proportional) with the cost of the intervention. Both objective functions need to be minimized. The results of the multi-objective optimization are Pareto fronts made up of solutions with N_{val} ranging from 0 to n_p. Optimizations run in this work were performed in the Matlab(R) 2018b environment by making use of a single processor of an Intel(R) Core(TM) i7-8750 2.20 GHz unit. EPA-SWMM was embedded in the structure of NSGA II for the network hydraulic simulation. Details on the two NSGA II-based optimization schemes developed are discussed as follows.

NSGA II with gate valves

The first optimization scheme considers installation of gate valves in the network pipes, as in the first SA algorithm described in sub-section 3.3.1. In other words, the scheme does not take into account the valve settings (the degree of closure) but only the place of installation within the network. The goal is to maximize the value of *UC* irrespectively of changes in nodal *SR* that may occur after the re-arrangement of the flow circulation in the network.

In this optimization scheme individual genes can take on two alternative values, 1 or 0, which indicate presence or not of the gate valve in the pipe, respectively. Penalties are assigned to those solutions representing valves configurations that cause topological

disconnection of network nodes. Solutions that eventually lead to overflow at the supply reservoir are also penalized in the GA code.

NSGA II with control valves

The second optimization scheme assumes installation of control valves in the network pipes, as in the second SA algorithm described in sub-section 3.3.1. Each valve can be set at a specific degree of closure rather than fully closed or fully open exclusively as proposed in the first problem setting. Placement of control valves in the WDS is carried out in order to maximize the value of *UC*, focussing also on the level of supply of individual network nodes. Specifically, decrease in the value of individual nodal *SR* below the threshold of equity *ET* of the network is not allowed by the algorithm. This means that, for each simulated scenario (i.e., any configuration of valves), nodal values of *SR* are compared with the original no-valve scenario. The algorithm assumes that nodes that originally have *SR* lower than *ET* must not further worsen their condition. On the other hand, it is allowed for nodes with *SR* higher than *ET* in the no-valve scenario to decrease their *SR* down to the *ET* value.

In this second optimization scheme, genes in the individual solutions can take on three possible values: 0, 1 or 2. Gene 0 stands for the absence of valve at the generic pipe. Genes 1 and 2 indicate the presence of a valve at the pipe with the valve partially open or fully closed, respectively. A sub-function within the algorithm was set-up to find the optimal settings for partially open valves (all genes 1). The

sub-function tries all the combinations that can be obtained from the initial set of K values provided as input to the algorithm. As an example, let us consider installation of 4 control valves in the WDS. Assuming a set of 3 K-values for each valve, the total number of combinations to explore for the detection of the best value of service equity is $3^4=81$. A database of the explored individuals is progressively updated during the running of the algorithm in order to avoid further simulations of individuals already analysed. Penalties are assigned as in the first optimization scheme. Further penalties are assigned to those solutions that do not respect the constraints regarding the nodal SR discussed before.

The simultaneous optimization of valve location and setting may result in an increased computational effort. For this reason, a second application of the optimization scheme was developed that allows reducing the size of the initial set of pipes that are potential candidates for the valve locations. Only valve locations that can be the most effective in changing the flow circulation in the WDS were considered (that is pipes that intercept significant flow). Specifically, the WDS need to be preliminary simulated in the no-valve scenario to evaluate pipe flows. Then, only pipes with flow larger than zero were included in the reduced set of potential locations for the valves for the application of the optimization scheme.

4. Application of the methodologies to case studies

The methodology described in chapter 3 was applied to different case studies. The first objective was to evaluate the potential of EPA-SWMM software in the simulation of intermittent WDSs. To achieve this objective, first the analysis focused on the network filling phase of water distribution networks. Case study 1 was identified for this specific objective. For this case study, the simulation results provided by EPA-SWMM were compared to experimental observations available from the field. Further experiments were carried out in another intermittent system (case study 2) in order to test the methodology in a more comprehensive way. In particular, the whole cycle of the intermittent water network was simulated with EPA-SWMM and the results were compared to the collected experimental data. Finally, another simple WDS (case study 3) was used for comparing EPA-SWMM and RWC model in reproducing the network filling process of intermittent WDS. Case study 3 was also used to test the efficiency of the proposed methodologies to improve equity in water distribution among users.

4.1. Case study 1. The WDS of Ragalna

4.1.1. Description of the network

The case study 1 water distribution network supplies water in Ragalna, a small municipality in south-eastern Sicily (Italy). The layout of the network is shown in Figure 1. The network is supplied by gravity through a single head tank with constant water level of 2.8

m. It was skeletonized by 55 demand nodes and 58 pipes. The characteristics of nodes (elevation *z*, and nodal demands) and pipes (length *L*, diameter *D*, and Strickler roughness coefficient *k*) are reported in the supplementary material (Tables ST1 and ST2, respectively). As shown in Table ST1, the network is characterised by high gradients in elevation: the difference in elevation between the source node (node 23) and the lowest node (node 8) is about 127 m and the range of pipe slopes varies between 1% and 23%.

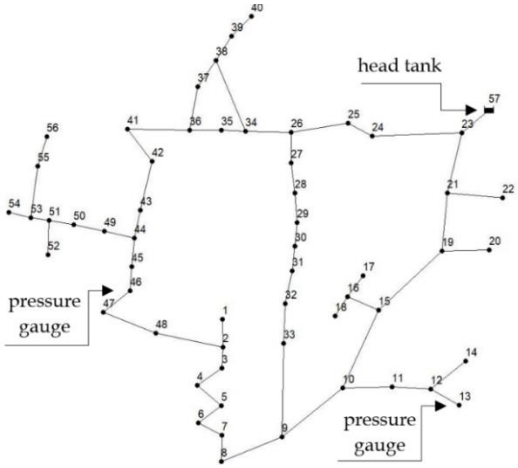

Figure 1. Case study 1. Layout of the network and sites of installation of the pressure gauges.

During a research program carried out in the month of October 2010 for monitoring the filling phase of the network, two pressure gauges (full-scale 25 bar, accuracy 0.1 bar) were installed in the district in order to obtain pressure measurements during the network operation. The demand at the nodes (reported in Table ST1) was estimated based on flow measurements. For this purpose, an

ultrasonic flowmeter (accuracy 0.5%) was installed at the head tank outlet. Arrows in Figure 1 indicate the sites of installation of the pressure gauges (close to nodes 13 and 46, respectively). Pressure measurements were acquired with a time granularity characterized by a 5 minutes time step. The network filling test started at 9:00 a.m. At that hour the network was empty.

The network simulation by EPA-SWMM was carried out assuming values of 5 m, 30 m and 0.5 for p_{min}, p_{req} and β, respectively (Eq. 6). Simulations were conducted assuming a maximum value of Δx=100 m. This determined that pipes with $L>\Delta x$ were segmented into sections of length ≤ 100 m. The chosen spatial scale value was proven to be sufficiently small to provide accurate results. In fact, further simulations with Δx equal to 50 m and 10 m returned almost identical model output in terms of accuracy of the results. The value of Δt was set to 10 seconds according to Eq. (10). The total duration of the simulation was 4 hours.

4.1.2. Results. Network filling process with EPA-SWMM

Application of EPA-SWMM to case study 1 allowed evaluating the suitability of the software for the simulation of the network filling process. Available field data were used to validate the model results. Figure 2 reports some of the results obtained using the model. In particular, the figure shows the comparison between numerical and experimental values of the pressure during the network filling process at gauged nodes 13 and 46, respectively.

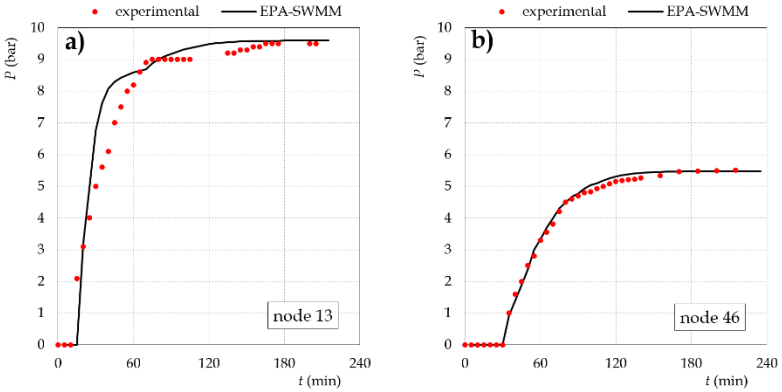

Figure 2. Case study 1. Measured and simulated pressure evolution at a) node 13 and b) node 46.

The model correctly reproduces the time the pressure starts to increase at both nodes. The analysis of the figure shows that the filling front reaches node 13 and node 46 in about 10 and 30 minutes, respectively.

Globally, also the rising trend of the pressure is well captured by the model at the two nodes with a pressure value at regime that is very close to the experimental one. Such a regime is shown in Figure 2 to be reached in about 2 hours from the beginning. However, differently from node 46 (for which an excellent matching of numerical and experimental pressure results was obtained), the model tends to slightly overestimate measured pressures at node 13 for pressure values above 4 bar. This behaviour would suggest underestimation in the value of the water demand at node 13 or a not appropriate evaluation of the parameters of Wagner's function for that node. Non-

uniform spatial distribution of water leakages in the network (not modelled for this case study) may also represent another potential reason of the different model ability in matching the experimental data at the two gauged nodes.

The negative impact of the intermittent supply is shown in Figure 3 with regard to the non-uniform distribution of the water resource both in time and in space. The figure reports (side to the node ID) the time tp_{min} in minutes (underlined numbers in red) needed to supply water at each demand node (when $p>p_{min}$).

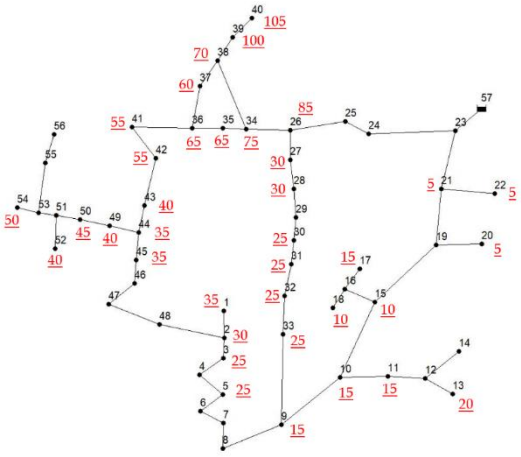

Figure 3. Case study 1. Values of tp_{min} (underlined numbers in red) at the different network demand nodes.

Results show an ample variation of tp_{min} in the range 5-105 minutes, therefore pointing out significant disparities in time of supply among users. The value of tp_{min} is significantly affected not only by the node

distance from the reservoir, but also by the node elevation. For example, Figure 3 highlights that some demand nodes (e.g. nodes 26 and 34) show very high values of tp_{min}, despite their proximity to the reservoir. The behaviour of these nodes was observed to be affected mainly by the low value of the reservoir water level, as well as by the high longitudinal slope of the downstream network, which in turn determined long-term free-surface flow condition (e.g. in pipes 34 and 35) during most of the duration of the filling phase.

Although Figure 3 revealed differences in the water supply timing at the various network nodes (thus potential disparities among the users of the water distribution service), it should be pointed out that such differences assume increased relevance for districts characterized by a short duration of the water supply period. Conversely, when the duration of the water supply period is sufficiently large, the impact of the filling phase on the water distributed to the users is relatively modest.

It should be stressed that simulations conducted with the RWC model revealed the inability of the approach to describe the filling process of the network because the basic assumptions of the RWC theory were not verified for case study 1. In particular, the output results of the RWC model returned unphysical values of pressure at nodes and velocity in pipes due to the high pipe slopes and to the low water head at the reservoir. For this reason, case study 1 was not used

for comparison of the simulation results of the two models (EPA-SWMM vs RWC model).

4.2. Case study 2. The WDS of Mirabella Imbaccari

4.2.1. Network description and monitoring campaign

A comprehensive campaign of monitoring was carried on another real intermittent WDS located in southern Italy with the objective to analyse the whole cycle of the intermittent system (filling phase, operation under pressure condition and emptying phase).

The WDS supplies water to the small municipality of Mirabella Imbaccari located in the internal areas of Sicily. The municipality has a resident population of about 5000 inhabitants. Floating population brings this number up to 7000-8000 during summer season (months of July and August). Available water sources for the WDS (water springs and wells) provide a total mean (in the year) flow of about 15-18 l/s. The network layout is shown in Figure 4.

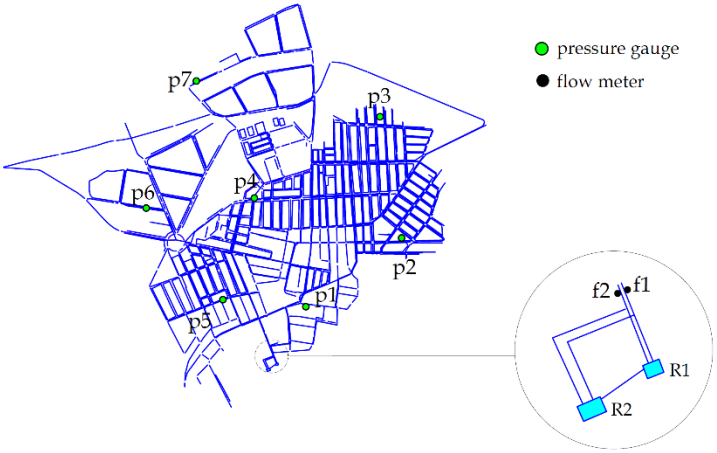

Figure 4. Case study 2. Layout of the network and site of installation of pressure gauges and flow meters.

The WDS is supplied by 2 reservoirs (R1 and R2 in Figure 4). Both reservoirs have rectangular bottom shape. In particular, R1 (elevation of 528 m s.l.m.) has a bottom surface area of about 193 m^2 and vertical sides of about 4.3 m. Reservoir R2 (elevation of 524.5 m s.l.m.) has a bottom surface area of about 208 m^2 and vertical sides of about 5.6 m. All the water coming from the available sources continuously supply reservoir R1 during the 24 hours of the day. A pipe located at 3.72 m from the bottom of R1 links the two reservoirs (that are in series) allowing excess water to overflow from R1 to R2. In this way, the R2 is filled only when R1 is full. As Figure 4 shows, each reservoir has two outlets (placed at 0.7 and 0.25 meters over the bottom of reservoir R1 and R2, respectively). The outlet pipes of R2 convey the flow in the

outlet pipes of R1 (one each); the last ones proceed downstream to feed the whole system. Gate valves are installed in the outlet pipes of both reservoirs (4 in total). Due to the age of the WDS and the lack of periodical maintenance operation, the network is characterized by a huge amount of water losses.

The network characteristics (nodes elevation, length and material of the pipes) as well as information about the distribution of the population in the area served by the WDS were obtained from both data provided by the municipality and the field investigation. Primary feeders pipes of the network (larger diameters) are in ductile iron while secondary feeders pipes (smaller diameters) are in HDPE. The network is characterized by high gradients in elevation with differences between the highest point (reservoir R1) and the lowest ones up to about 100 m. The whole area covered by the WDS can be divided into 2 different altimetric zones: an "high zone" (south-east part of the network in the figure) and a "low zone" (north-west part). A pipe just downstream the two reservoirs connects the high zone of the network to the low one. A gate valve installed in the connection pipe can be closed to hydraulically divert flows and or disconnect the two parts of the network, if needed.

The WDS of Mirabella Imbaccari historically provides water to consumers intermittently. For this reason, almost all households are equipped with private tanks in order to collect water during the supply hours. These back-up facilities allow users to have access to

water even after the interruption of the supply from the reservoirs. Most of the private tanks are located on the rooftop terraces of the houses. Only few of them are basement tanks. The management of the supply period by the municipality slightly varies during the months of the year and the days of the week. However, generally, water is provided to users according to the following schedule. In the morning (6-7 a.m.) first, the gate valves in the outlet pipes of reservoir R1 are opened. After about 3.5-4 hours from the beginning of the supply period (approximately when water level inside R1 drops to 1-2 m) gate valves in the outlet pipes of R1 are closed while those of R2 are opened. Accordingly, in this second part of the supply period, water is supplied only from reservoir R2 while R1 is progressively refilled by to the inflow from the sources. During the afternoon (between 12 and 4 p.m.) gate valves of the outlet pipes of R2 are closed and the supply period of the day is over. Generally, in the first 1-2 hours of the supply period the gate valve in the pipe connecting the high zone of the network to the lower one is maintained closed to assure suitable pressure in the "high zone". Then, the gate valve is opened, and the flow is also diverted to the part of the network at lower elevation.

A monitoring campaign of the WDS operation was conducted during the summer season of year 2019. In Figure 4 the installation points of the measurement devices are highlighted. In particular, two electromagnetic flow meters (model RPmag, range 0.1-110000 m^3/h) were installed in the outlet pipes of reservoir R1. The position of the flow meters allows measure the flow coming from both reservoirs.

Seven pressure gauges (model Pedrollo MR10, range 0-10 bar) were installed throughout the network. Gauges from 1 to 3 were installed in the high zone of the network while gauges from 4 to 7 were installed in the low zone.

Totally, 8 days of experiments were carried out from June to August 2019 (2 days on June, 3 days on July and 3 days on August) covering different days of the week in order to catch weekly variations on consumer habits and managing strategies of the WDS. Moreover, due to the floating population on summer season, the number of consumers served by the WDS potentially grew during the period of time covered by the measurement campaign, with a peak of population in August.

In each day of measurements (generally from 6 a.m. to 6-7 p.m.):

- the outflow from the reservoirs was continuously measured by the flow meters and data were stored in a datalogger with a time step of 1 minute;
- daily mean inflow (from water sources) to reservoir R1 was evaluated based on a set of volumetric measurements;
- water level inside the reservoirs were measured with a time step of about 1 hour;
- nodal pressures at the 7 pressure gauges were collected approximately every hour;
- modalities and times of opening and closure of gate valves in the WDS were recorded.

4.2.2. Modelling of the WDS with EPA-SWMM

EPA-SWMM model of the WDS of Mirabella Imbaccari was built. The network was skeletonized in 922 nodes and 1073 pipes. The collected experimental data were used for the calibration of the model.

Information about inhabitants, collected through population census, were aggregated at the scale of district. In particular, the network was divided into 361 districts. Private tanks interposed between the network nodes and the users were modelled by using Eq. (7). A configuration typical of tanks installed by households of intermittent WDSs in Italy (i.e., assuming one cube-tank of 1 m^3 capacity for a 4-people household) was considered. Implementation of the hydraulic model of the WDS was carried out through adoption of "equivalent" tanks that were used to simulate groups of private tanks belonging to the same district of the network. Therefore, 361 equivalent tanks (one per district) were globally considered. Their capacity was calculated based on the total population of the corresponding district. Resulting equivalent tanks are all 1-meter tall with variable bottom surface area according to the served population. The elevation of the single equivalent tank was set computing the average elevation of the tanks of the corresponding district. The float valve controlling the inflow was assumed on the top of each equivalent tank. Values of 0.8 m and 1 m were considered for H_{min} and H_{max} in Eq (7), respectively. Therefore, inflow to the equivalent tank is restricted when the tank water level is 0.8 m while inflow stops when the water level achieves 1 m. Values of the other parameters in Eq. (7)

were chosen according to the experimental findings by Criminisi *et al*. (2009), De Marchis *et al*. (2014; 2015). The inflow to each equivalent tank was calculated by summing contributions of all the private (household) tanks belonging to the corresponding district of the network (by use of Eq. 7). With the tank interposed between the user and the network node, demand consumptions are modelled as follows. As long as there is sufficient water inside the tank, the outflow from the tank is governed by the users' needs, as if they were not affected by the water scarcity scenario. A per capita water demand of 150 l per habitant per day was considering as suggested by Milano (2012) for small municipality. Therefore, the outflow from equivalent tanks is modelled by summing this per capita need for all the users of the corresponding district and by using the diurnal pattern reported in Figure SF1. Conversely, if the tank is empty, there is not outflow from the tank.

Water leakages were also modelled at the scale of district using Eq. (9). Therefore, 361 leakages points have been uniformly distributed in the network model.

Simulations were carried out by giving as input to the model the initial water level at both reservoirs at the beginning of the supply period and the inflow to reservoir R1. Instead, the outflow from the reservoirs and the pressure trend in the gauged nodes are the model output to be compared to experimental observations. Calibration parameters for the model are the initial water level inside the users'

tanks, the pipes roughness, the coefficient a and the exponent γ in the water leakages formulation (Eq. 9).

4.2.3. Results. Analysis on experimental data

The experimental campaign conducted on the network of case study 2 allowed to point out the operation of the WDS. Information provided by the water service company of the municipality during the monitoring campaign were also useful to better understand the system behaviour.

As explained in sub-section 4.2.1., the whole network is supplied through the two outlet pipes of reservoir R1. These pipes collect water coming from both reservoirs (Figure 4). However, because of the network layout, the flow is not equally distributed between the two outlet pipes. In particular, field surveys revealed that the outlet pipe in which flow meter f2 is installed serves a small loop of the network with low density of population. This loop extends in the "high zone" of the network. The rest of the network is basically supplied starting from the other outlet pipe (in which flow meter f1 is installed). The long-term analysis of data collected by the two flow meters confirms that the outlet pipe on the right conveys almost the totality of the water flow coming from the two reservoirs. For example, in Figure 5 the flows Q in the two outlet pipes of R1 as measured by the two flow meters is reported. Data are referred to a 1-week time window, from Monday February 17th to Sunday February 23rd, 2020.

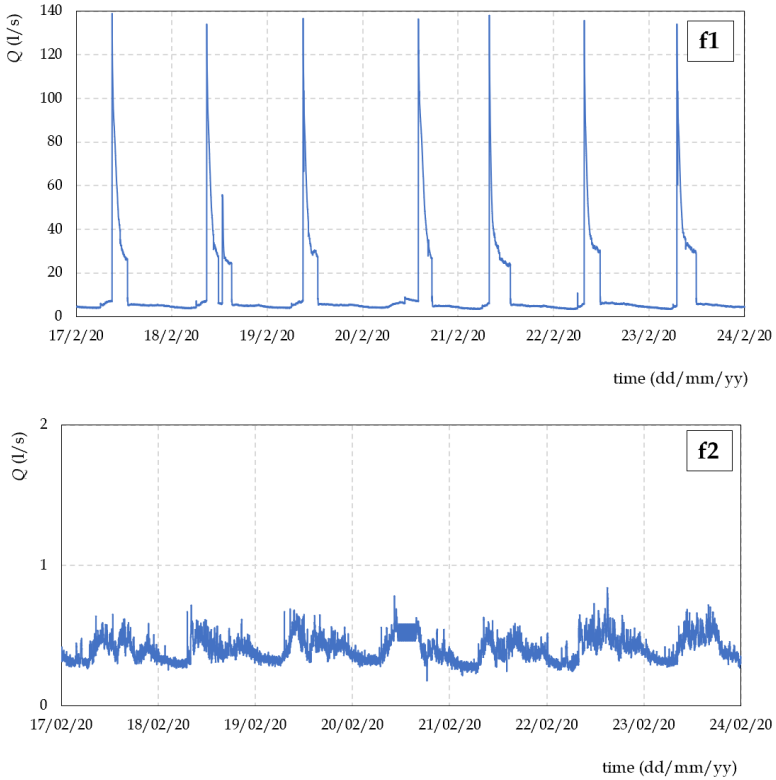

Figure 5: Case study 2. Flows *Q* as measured by the two flow meters in the period February 17th – February 23rd, 2020.

The figure highlighted the non-equal distribution of the flow in the two outlet pipes. As shown in the figure, the flow recorded by f2 oscillates around an average value of 0.4 l/s. On the other hand, flow meter f1 records the most important part of the flow during the supply period of each day. In particular, for the analysed week, f1 records a daily peak flow (about 140 l/s) at the beginning of the supply period

(instantaneous opening of gate valves in the outlet pipes of R1) followed by few hours (6-8) of average flow of about 30 l/s.

Another interesting point that can be observed from Figure 5 concerns the non-supplying hours. As discussed with the water company and observed during the field survey, gate valves in the outlet pipes of reservoir R2 do not work properly. In particular, they do not allow the full closure of the pipes, thus allowing some water to flow out from reservoir R2 also during non-supplying hours (after the closure of all gate valves downstream the two reservoirs). Figure 5 actually shows that the flow recorded by both flow meters never goes to zero as it should be expected in an intermittent system during non-supply hours. Analysis of the time series recorded by f1, provides identification of the exact time at the end of the supply period in which the gate valves are closed (vertical lines in the graph with the flow going down to a minimum value between 7-10 l/s until the re-start of the supply period on the next day). This minimum flow is exclusively due to the gate valves in the outlet pipes of R2 that remain a little bit open. Regression on experimental data allowed to find a linear relationship between the flow recorded by the flow meter during the non-supply hours and the water level inside reservoir R2. This relationship has been used in the next steps of network modelling to describe the outflow from R2 during the non-supply period of the day. As a consequence of this continuous minimum flow all the night long, most of the user's private tanks are full at the beginning of the next supply period in the morning. Another important consideration that

derives from observation of Figure 5 is that the supply period covers less than 1/3 of the day, ranging from 5 to 7 hours per day.

Preliminary analysis of experimental data collected during the days of the experiments also allowed to study the process of filling of reservoir R2 through the overflow pipe connecting R1 and R2. The mass balance of the two reservoirs allowed to highlight that the flow $Q_{R1\text{-}R2}$ from R1 to R2 can be well described by the following relationship:

$$Q_{R2\text{-}R1}=C\cdot A_p\cdot\sqrt{2g(H1-h_p)} \tag{15}$$

where C is a non-dimensional outflow coefficient, A_p is the wetted area of the pipe connecting the two reservoirs, $H1$ is the water level inside reservoir R1 and h_p=3.72 is the elevation of the pipe from the bottom of R1. Value of C=0.4 properly describes the mass balance of the reservoirs. Even this relationship has been embedded in the network model described in the next sub-section.

4.2.4. Results. EPA-SWMM model calibration

In the following sub-section results of the simulation with the software EPA-SWMM are presented. The simulation concerns the day of the experiments carried out on Sunday 16th June 2019. Early summer in Mirabella Imbaccari is not interested by significant fluctuant population so that only the residential population (5017 habitants) was considered in the model.

The monitoring of the WDS operation pointed out that on such a day the supply period started at time 06:07 a.m. with the opening of gate valves of reservoir R1. After 3.5 hours of supply from R1, at time 09:38 a.m. the operators closed the gate valves of R1 and opened those of R2. The supply period continued for just over 2 hours from reservoir R2. At time 11:50 a.m. gate valves in the outlet pipes of R2 were closed and the supply period was over. The gate valves in the diversion pipe between the high and the low zone of the network remained open during the whole supply period. This type of operation of the WDS is typical of weekend days when the water service operators at work are few. As explained in sub-section 4.2.1., during weekdays this gate valves remains closed in the first part of the supply period to allow the re-filling of users' tanks in the high zone of the network with suitable values of pressure.

In Tables 1 and 2 the field measurements (water level *H1* and *H2* in the reservoirs and pressure *P1* to *P7* at the gauged nodes, respectively) collected on the considered day are reported.

Table 1: Case study 2. Experimental water level *H1* and *H2* inside reservoirs on 16th June 2019.

time (hh:mm)	***H1* (m)**	**time (hh:mm)**	***H2* (m)**
06:07	3.69	06:12	4.93
06:45	2.99	06:50	4.93
07:45	2.53	07:50	4.93
08:45	2.18	08:50	4.82
09:38	1.93	09:50	4.82
10:45	2.22	10:50	4.43
11:45	2.54	11:50	3.80
12:45	2.95	12:50	3.40
13:45	3.26	13:50	3.13
14:45	3.53	14:50	3.13
15:52	3.88	15:50	3.03
16:45	3.90	16:50	3.00
17:45	3.93	17:50	3.16
18:45	3.93	18:50	3.18

Table 2: Case study 2. Experimental pressure *P1*, *P2*,…,*P7* at the gauged nodes on 16th June 2019.

time (hh:mm)	P1 (m)	time (hh:mm)	P2 (m)	time (hh:mm)	P3 (m)	time (hh:mm)	P4 (m)
07:01	16.21	07:03	27.53	07:04	30.08	07:07	38.75
08:03	20.19	08:04	26.51	08:06	27.53	08:09	42.93
08:55	18.35	08:58	25.49	08:59	28.45	09:02	42.83
09:53	16.32	09:55	22.94	09:57	24.47	10:00	41.81
10:57	15.30	10:59	21.41	11:00	24.57	11:03	41.30
11:59	10.10	12:01	16.42	12:03	16.32	12:06	16.32
12:57	10.30	12:58	15.30	13:00	15.30	13:03	0.00
14:04	10.10	14:06	15.81	14:08	16.21	14:09	0.00
14:57	10.20	14:59	16.32	15:02	17.13	15:03	0.00
16:05	10.20	16:07	16.32	16:09	17.13	16:10	0.00
16:54	10.20	16:56	16.21	16:58	16.32	16:59	0.00
17:56	10.20	17:58	16.32	18:00	16.32	18:01	0.00
18:55	10.10	18:57	16.11	18:59	15.30	19:00	0.00
time (hh:mm)	**P5 (m)**	**time (hh:mm)**	**P6 (m)**	**time (hh:mm)**	**P7 (m)**		
07:09	53.13	07:11	61.69	07:14	75.56		
08:10	54.04	08:12	62.20	08:16	51.49		
09:04	53.53	09:06	61.28	09:09	66.28		
10:02	51.49	10:04	61.18	10:07	71.38		
11:05	50.88	11:07	59.14	11:11	65.26		
12:08	24.47	12:10	34.67	12:13	52.92		
13:05	20.29	13:06	30.49	13:10	48.95		
14:10	19.88	14:12	30.39	14:15	46.91		
15:04	18.35	15:06	28.55	15:09	46.91		
16:11	18.35	16:12	28.55	16:16	46.91		
17:00	17.33	17:02	26.61	17:05	46.91		
18:02	16.32	18:04	26.41	18:07	42.32		
19:01	12.24	19:03	20.90	19:06	40.89		

The table highlights that from 6 a.m. to 7 p.m. field measurements were acquired approximatively every hour starting from water levels in reservoirs R1 and R2 and then proceeding with pressure at the gauged nodes in the sequence from 1 to 7. Measurements of water level at reservoirs and pressure at nodes were carried out for several hours after the end of the supply period, in order to catch the behaviour of the WDS during all its functioning phases.

The simulation with EPA-SWMM of Sunday 16th June 2019 was run from 6:07 a.m. (beginning of the supply period) to 7:30 p.m., thus covering all the time window of experimental data. The calibration of the model led to set values of parameters as discussed in the following. In line with experimental observations as discussed in the previous sub-section, water level inside all the users' tanks was set at its maximum value of 1 m (i.e., the tanks were considered to be full at the beginning of the supply period). . Values of 6×10^{-4} and 1.18 were set for parameters a and γ in the water leakages formulation (Eq. 9), respectively. With regard to values of pipe roughness, Manning's coefficients of 0.0143 and 0.01 were set for pipes in ductile iron and HDPE, respectively. These values are commonly used in literature for such pipe materials. The head loss coefficient (Eq. 8) for the gate valve in the pipe connecting the high and the low part of the network was set to K=10. The comparison between simulated and experimental data for the water level at the reservoirs and pressure at the 7 gauged nodes is reported in Figure 6 and Figure 7.

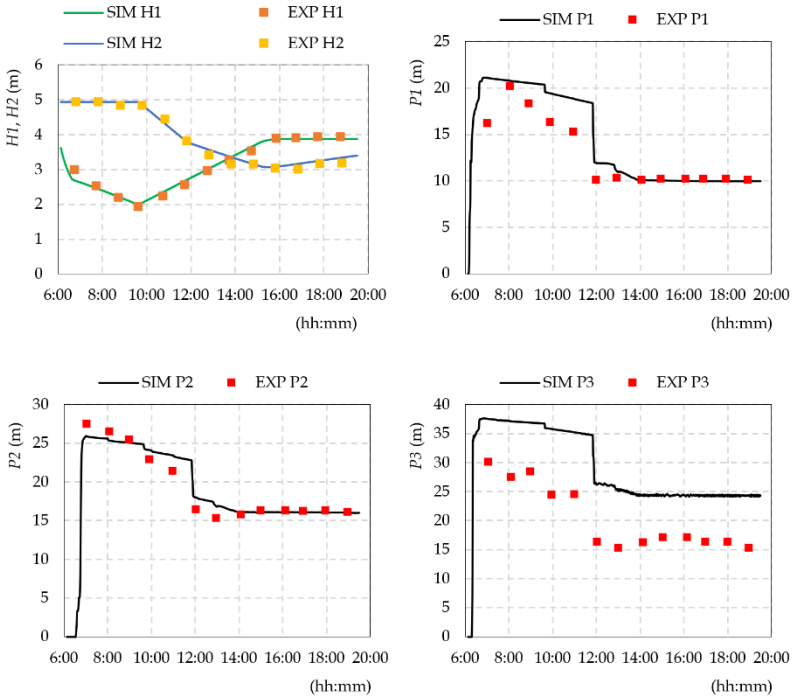

Figure 6: Simulated VS experimental water level *H1* and *H2* inside reservoirs and pressure *P1*, *P2* and *P3* at gauged nodes for 16th June 2019.

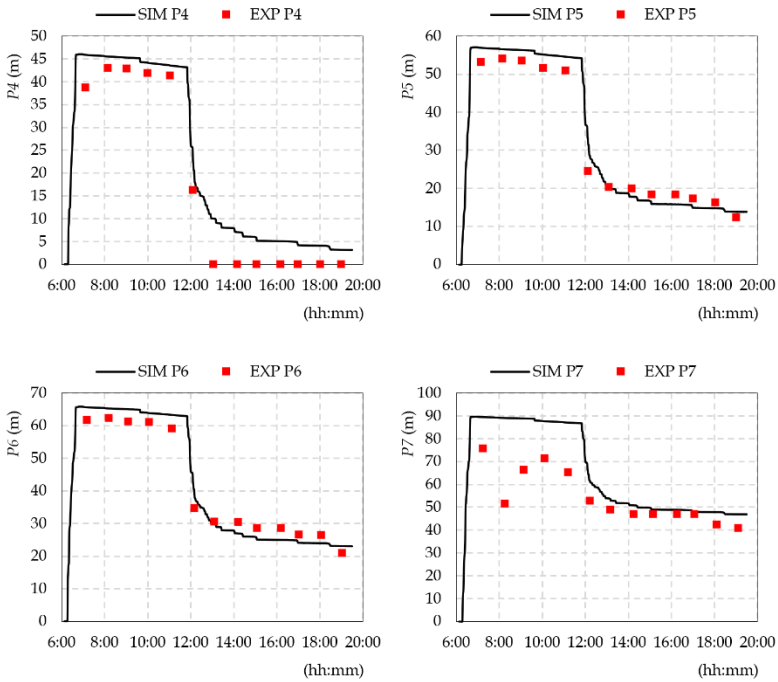

Figure 7: Simulated VS experimental pressure *P4*, *P5*, *P6* and *P7* at gauged nodes for 16th June 2019.

First graph in Figure 6 shows a very good agreement between simulated and experimental water levels at R1 and R2 pointing out that EPA-SWMM correctly describes the inflow/outflow balance of the reservoirs. At the beginning of the supply period a quick emptying of reservoir R1 can be observed with water level reducing from 3.69 (06:07 a.m.) to 1.93 meters (09:38 a.m.). In the meanwhile, water level inside R2 remains almost constant. The Figure shows also that, starting from 09:38 a.m. the network is supplied by reservoir R2, so that water level *H2* decreases while *H1* increases because reservoir R1

has now only the inflow component from the sources. Interestingly, a change in the slope of the decreasing curve of water level H2 can be observed in the graph. The point of slope variation corresponds to the closure of gate valves in the outlet pipes of reservoir R2 (11:50 a.m. i.e., end of supply). The curve passes from a high slope to a lower one. The graph shows that EPA-SWMM software reproduced reliably the described variation in the slope of *H2* curve. Finally, around 4 p.m. water level inside reservoir R1 reaches the elevation of the overflow pipe (3.72 m) so that all the incoming flow to R1 overflows to R2. Therefore, in the final part of the graph, water level inside R2 increases (being the inflow from R1 larger than the outflow) while that in R1 remains almost constant.

As regards the other graphs in Figures 6-7, a peculiar pressure trend can be observed for all the gauged nodes. Two distinct phases of the day can be individuated: the first characterized by higher pressure values and the second by lower ones. As expected, the drop of the pressure values corresponds to the end of the supply (around 12 a.m.) for all the monitored nodes. Gauged nodes from 1 to 3 (Figure 6) are in the high zone of the network and show maximum pressure values during the supply period between 20 and 40 m. Gauged nodes from 4 to 7 (Figure 7) are in the low zone of the network with maximum pressure values up to 90 m for the lowest node (7). The comparison between simulated and experimental data shows that EPA-SWMM is generally able to describe this 2-phases pressure trend at the monitored nodes. Going into details of the single pressure

gauge, for some nodes (2, 5 and 6) simulated pressure values match experimental data quite good in both phases of the day. For gauged node 3, instead, EPA-SWMM overestimates pressure values of about 5 m during the supply hours and of about 10 m during the non supply hours. Gauges 1 and 7 also show an overestimation of pressure values by EPA-SWMM mainly during the supply hours. Finally, for gauged node 4 simulated pressure values are higher than experimental ones in the second part of the day. These discrepancies between simulated and experimental data (with EPA-SWMM always overestimating pressure values) are probably to be ascribed to local head losses due to unknown singularities throughout the network. For example, the fact that for gauged node 4 zero pressure values were recorded during the non-supply hours while the other monitored nodes (in the same elevation zone of the network) show values of pressure between 20 and 50 m, could be explained with the presence of oversized users' tanks in that area or exceptional users' demand in the particular analysed day. This hypothesis is also in line with field surveys. Therefore, different tanks' size for different parts of the network could be considered in the model for future simulations. The overestimation of simulated pressure values for gauged node 3 (with nodes 1 and 2 in the same elevation area of the network showing a good agreement between simulated and experimental data) could be related to old devices (still in place but no more in action) or other local singularities that determine a general head losses in the area of node 3.

In order to evaluate the sensitivity of some of the main parameters used for the simulation, a sensitivity analysis was carried out. The initial water level inside private tanks has a great impact on the mass balance of the reservoirs. Simulations with initial water level inside private tanks ranging from 0.5 to 1 m were carried out. As an example, in Figure 8 the comparison between simulated and experimental *H1* and *H2* for the initial water level in private tanks of 0.8 meter is reported. The values of the other parameters are left unmodified.

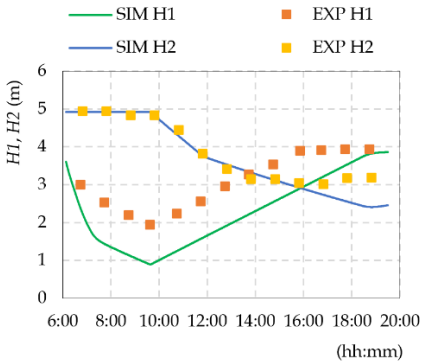

Figure 8: Simulated VS experimental water level *H1* and *H2* inside reservoirs for initial water level inside users' tanks of 0.8 m.

As shown in the figure, EPA-SWMM performs an excessive initial emptying of reservoir R1 as compared to experimental data because more water is requested by the network for the filling of the private tanks partially empty. Water level inside R1 reaches a minimum value of about 1 m at 09:38 (almost 1 meter under the corresponding experimental value). As expected, assumption of the private tanks

partially empty generates a peak demand at the beginning of the supply period. Even simulated curve for water level inside reservoir R2 shows a sharper decrease of *H2* for the part of the day after 4 p.m. In fact, due to the initial excessive emptying reservoir R1 overflows to R2 at 6.20 p.m. instead of 4 p.m. as in the previous simulation. Therefore, the flow from R1 to R2 and the consequent re-filling of R2 starts later. Even the match with experimental data for simulated pressure at the gauged nodes is globally worse for this simulation as compared to results provided in Figure 6-7.

As regards the coefficients in the leakages formulation (Eq. 9), simulations with a in the range 10^{-4} - 10^{-2} and γ between 0.5 and 2.5 were carried out (Farley & Trow 2003; Al-Ghamdi 2011; Ferrante 2012). As an example, in Figure 9 the comparison between simulated and experimental *H1*, *H2* and *P2* for simulation with a=10^{-4} is reported. The values of the other parameters are left unmodified.

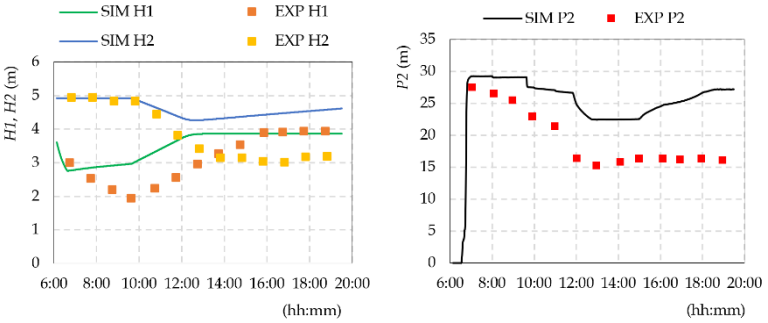

Figure 9: Simulated VS experimental water level *H1* and *H2* inside reservoirs and pressure *P2* for coefficient a=10^{-4}.

The figure shows that both reservoirs in EPA-SWMM empty less than they actually do according to experimental data, highlighting a decreased network water request. As expected, the reduced magnitude of the water leakages volume leads to overestimate the simulated water level *H1* and *H2* for all the duration of the simulation. Interestingly, minimum water level inside R1 (slightly less than 3 m) is reached around 6:30 a.m. (before the time of closure of gate valves of R1), thus pointing out that the outflow from R1 is even less than the inflow from the sources. The reduced magnitude of water leakages also determines a general increase in nodal pressure values throughout the network, as testified by the graph in Figure 9 for gauged node 2. Values of simulated pressure are higher than experimental ones both during the supply hours (until 11:50 a.m.) and after the end of the supply period. Simulated pressure P2 even shows an increasing trend starting from 3 p.m. Such an increase was not observed experimentally.

Finally Figure 10 reports the comparison between simulated and experimental *H1*, *H2* and *P6* for simulation with exponent $\gamma=2$ in the leakage formulation. As before, the values of the other parameters are left unmodified.

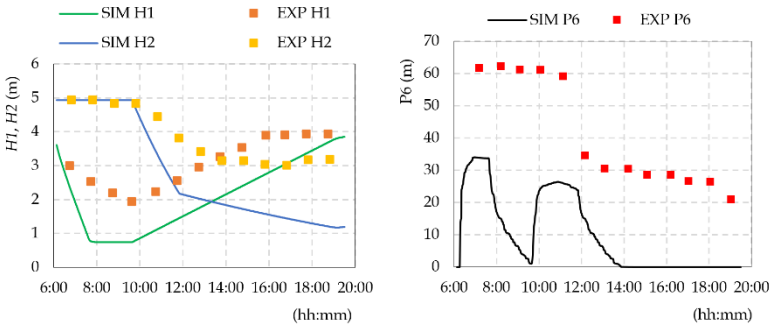

Figure 10: Simulated VS experimental water level *H1* and *H2* inside reservoirs and pressure *P6* for exponent γ=2.

The figure shows that EPA-SWMM performs the total emptying of reservoir R1 because of the increased water leakages volume. In fact, water level inside R1 quickly reaches the minimum value of 0.7 m (distance of the outlet pipes from the bottom of the reservoir). Even the value reached by R2 at the end of the supply period (11:50 a.m.) is significantly lower (about 2 m) than the experimental one. Interestingly, after the end of the supply, water level inside R2 continues to decrease because there is no inflow to the reservoir. In fact, water level inside R1 reaches the elevation of the overflow pipe only at the end of the simulation. As opposite to previous simulation (Figure 9), the increased magnitude of water leakages determines a general decrease in nodal pressure values throughout the network, as testified by the graph in Figure 10 for gauged node 6. EPA-SWMM underestimates pressure at node 6 of about 30 m in both phases of the day (supply and no-supply period). A quick drop of the nodal

pressure value before 10 a.m. is even reproduced by EPA-SWMM. Such trend is not supported by experimental observation.

Globally, EPA-SWMM results confirm the ability of the software in the modelling of intermittent WDS. In addition to case study 1 for which only the filling phase was simulated, the results shown in this sub-section highlight the possibility to model the whole cycle of complex intermittent WDS, considering also private tanks interposed between users and the network nodes. With a proper calibration of the model parameters, results of the simulation with EPA-SWMM showed a very good agreement with experimental data. Moreover, the software was able to simulate the different phases of the WDS operation, correctly reproducing water level inside reservoirs and nodal pressure at the gauged nodes both during supply and non-supply hours. Future steps of the research should involve the refined description in EPA-SWMM of the network, including modelling of local singularities eventually identified after further field surveys. Moreover, simulations of the other measurement days would allow to improve the model calibration. Finally, simulation with different values of the parameters for different part of the network could allow to better catch the WDS behaviour in the two zones a different elevation.

4.3. Case study 3. The WDS of Castelfranco Emilia

4.3.1. Description of the network

The WDS considered as third case study supplies water to Castelfranco Emilia, a small village in northern Italy. The network (Figure 11) has been used in the literature for the analysis of demand and leakages in WDSs (Farina *et al.*, 2014; Creaco and Walski, 2017) and it consists of 26 nodes (of whom 25 are demand nodes), one source node (supply reservoir), and 32 pipes in PVC. The nodes of the network are at the same elevation, 35 m below the source node. The network daily average demand is equal to 50.49 l/s. Table ST4 and ST5 in the supplementary material provide nodal average daily demands and characteristics (length, diameter and roughness) of the pipes (Creaco and Walski, 2017). All pipes are assumed to have a Manning roughness coefficient value of 0.01 s/m$^{1/3}$ (typical value for PVC pipes).

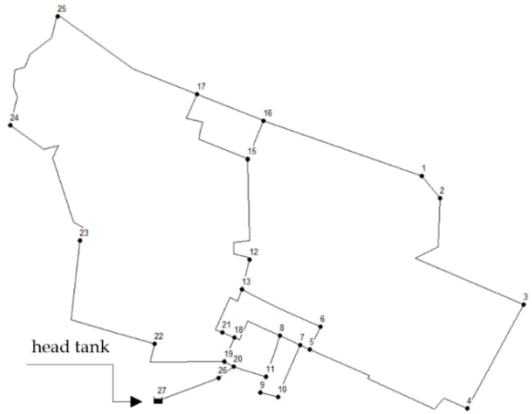

Figure 11. Case study 3. Layout of the network.

4.3.2. Network filling with EPA-SWMM and RWC model

Because of the characteristic flatness, the network is suitable for the application of the model based on the RWC theory. For this reason, case study 3 was used for comparison of the filling process as simulated by EPA-SWMM and the RWC model. As regard Wagner's function parameters (Eq. 6), values of 10 m, 30 m and 0.5 were assumed for p_{min}, p_{req} and β respectively (Ciaponi and Creaco, 2018). Values of Q_{req} at the different hours of the day were evaluated according to the demand pattern proposed by Creaco and Walski (2017) and reported in Figure SF1 in the supplementary material. From the operational point of view, the network was assumed to be filled starting at 6:00 a.m. and to be empty at the beginning of the simulation. Analogously to the case study 1, EPA-SWMM was applied assuming a maximum value of Δx=100 m which was preliminary observed to provide accurate simulation results. Use of Eq. (10) returned a time step Δt=5 seconds for the analysed network. The total duration of the simulation was 2 hours.

4.3.3. Application of algorithms to improve equity in water distribution

The simple network of case study 3 (Figure 11) was also used for testing algorithms described in section 3.3. Network users are supposed to be equipped with private tanks under the hypothesis of water shortage scenario. EPA-SWMM was used for the network hydraulic simulation in all potential configurations of valve installation. Private tanks interposed between the network nodes and

the users were modelled in EPA-SWMM as explained in sub-section 4.2.2. for case study 2. Being the network considerably smaller as compared to case study 2, the process of users aggregation for the modelling of equivalent tanks was conducted at the scale of the single demand node. Therefore, 25 equivalent tanks (one per demand node) were globally considered. Their installation was assumed 1 meter below the ground level (typical configuration in north Italy), and their capacity was calculated based on the total population supplied by the corresponding network node. As for case study 2, values of nodal average daily demands in Table ST4 and the diurnal pattern reported in Figure SF1 were used to model the outflow from the equivalent tanks.

Conditions of water supply rationing due to water shortage were considered. Both modalities of intermittent water management described in the introduction are common in Italy. In many cases water managers opt for supplying a fraction of the water demand continuously for the 24 hours. This is the modality of supply management considered for case study 3. The amount of water continuously released from the supply reservoir was assumed equal to 70% (35.34 l/s) of the total daily demand. Under the depicted scenario the equity threshold ET introduced in section 2.2. is equal to 0.7. Therefore, equitable management of the available water resource would assume that nodes showing $SR>0.7$ should reduce their supply to users in favour of those nodes that have $SR<0.7$.

Simulations with EPA-SWMM of each configuration of valves in the WDS were carried out assuming the network pipes (as well as the equivalent tanks) to be empty at the beginning of the simulations. This condition allows considering heavy scenarios of water shortage (e.g., the restart of the system supply after the occurrence of a malfunctioning of the pumps at the source reservoir).

Moreover, EPA-SWMM was applied assuming a maximum value of Δx=100 m (as described in sub-section 4.1.1) for all the simulations carried out with SA algorithms. Such a spatial discretization was removed for the analysis conducted with the GA in order to reduce the computational effort. In fact, a very high number of network simulations have to be run for each generation of the GA. Therefore, a simplification of the model was necessary at the expense of a less accuracy in the simulation results.

4.3.4. Results. EPA-SWMM vs RWC

The characteristics of the third case study make the network suitable for the application of the RWC model, thus enabling the comparison of this model with EPA-SWMM. The comparison of the two models is shown, for example, in the graphs of Figure 12 in terms of both pressure (Figures 12a and 12b) and supplied flow (Figures 12c and 12d) at two nodes of the network during the process of filling of the network. In particular, the two nodes 13 and 24 were selected as representative of nodes close and far from the reservoir, respectively.

Figure 12 shows that the time evolution of the piezometric height at node 13 was reproduced by the two models in a similar way. Differences on the time the node pressure starts to increase due to the water front arrival are relatively small (about 2.5 minutes). Also, the general trend of pressures reproduced by the two models during the whole simulation is relatively similar, with the initial stage characterized by a sudden pressure rising and a smoother increase in the following phase, up to the achievement of the regime pressure. Conversely, larger discrepancies between the results of the two models were obtained for node 24 that is far from the source.

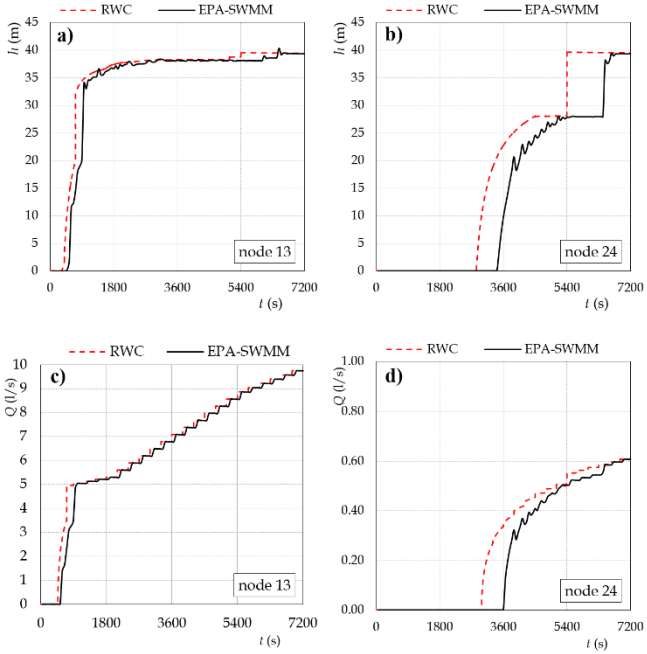

Figure 12. Case study 3. Time evolution of a), b) piezometric height *h* and c), d) supplied flow *Q* at node 13 and node 24, respectively.

In fact, although pressure-time curves are consistent, a marked offset in time axis is observed, clearly pointing out different times needed by the water front to achieve the node with the two models (47 and 56 minutes with the RWC model and EPA-SWMM, respectively). Generally, in comparison to EPA-SWMM, the RWC model overestimates the propagation velocity of the filling water front for all the nodes of the network (on average, for all the network nodes, the wave front calculated by the RWC anticipates EPA-SWMM of about 5 minutes). As expected, according to Eq. (6), the results of Figures 12c), d) show also underestimation of the time needed for the start of the supply (the nodal supply is anticipated) by the RWC model as compared to EPA-SWMM.

As a further analysis of the results, Table 3 reports the comparison of the two models for those pipes where the filling process simultaneously occurs from both pipe ends. The table shows the pipe section where the two approaching flow columns meet one each other (distances L_{SWMM} and L_{RWC} from the pipe end node). The table also reports the difference (in percent) between L_{SWMM} and L_{RWC} as obtained with the two models, showing values in the range 1.4-4.1%.

Table 3. Case study 3. Pipes filled by both ends.

pipe	L (m)	from node	L_{SWMM} (m)	L_{RWC} (m)	$(L_{SWMM} - L_{RWC})/L$ (%)
4	2851.4	1	800	757	1.5
8	817.4	10	340	314	3.2
9	1269.8	6	400	352	3.8
11	628.3	8	180	206	4.1
29	2452.7	25	400	435	1.4

Finally, the simulation with the two models globally provided the results reported in Table 4 in terms of total time to fill the network and total water volume supplied to users during a 2 hours period. In agreement with Figure 10, the results of the simulations confirm the filling process obtained with the RWC model to be significantly shorter than EPA-SWMM (about 15% less). Notwithstanding this, the volume supplied to users simulated with the two models is very similar (about 2.6% difference).

Table 4. Case study 3. Filling time and total volume supplied to users in the two models.

Model	Network filling time (h)	Total volume supplied to users (m^3)
RWC model	1.5	266
EPA-SWMM	1.77	259

The results of the simulations reported above point out the different ability of the two models to reproduce the filling process in

intermittent WDSs. Remarkably, the used model based on the RWC theory was not able to reproduce the filling process for the first case study network that is characterized by relevant longitudinal slopes of the pipes and low available water head at the reservoir. Conversely, EPA-SWMM was proven to provide results in good agreement with data available from field experiments carried out in the network.

The simulations have confirmed the possibility to compare the two models when the basic hypotheses of the RWC theory are valid. Interestingly, the results of the comparison carried out for the flat network of case study 2 pointed out that the two models allow reproducing the filling process in a similar way, at least in the part of the network close to the reservoir. This result is in agreement with the experimental findings by Guizani *et al*. (2005), that showed the flow column to be able to proceed with a quasi-vertical front in the pipes of the upstream part of the network. Instead, differences between the two models are observed as the distance from the source increases due to the increase of the energy losses. As Figure 12 shows, the pressure rising curves for the nodes far from the source have almost the same trend for both EPA-SWMM and RWC model, so that the discrepancy only consists in the temporal offset of pressure values. Future studies on the filling process could involve the comparison of EPA-SWMM results with the improved version of the RWC model proposed by De Marchis *et al*., (2010).

4.3.5. Results. Optimal valves location to improve equity

Behaviour of the network in the no-valve scenario

The case study network was preliminary simulated in the actual scenario without valves. The simulation of this scenario allowed defining a benchmark for the solutions provided later by the optimization algorithms. A first pressure-driven simulation (Eq. 6) was carried out without including equivalent tanks in the layout of the WDS. The results revealed that this configuration provides SR=0.7 at the condition of regime for all the network nodes. This means that, although stressed by water rationing conditions, the network without private tanks would provide maximum equity in water distribution among the users (UC=1). This result is clearly ascribed to the flatness of the network and to the small slope of the energy line allow equal withdrawal conditions at all the nodes of the WDS.

Unsurprisingly, when private tanks are installed by the users, the equity level decreases. Indeed, the results of a further simulation including the equivalent tanks in the layout provided nodal SR at regime reported in Table 5, showing a very low level of uniformity in water distribution. The table highlights that 13 nodes out of 25 do provide full satisfaction of the users' demand (i.e., SR=1.0), while users of 7 nodes do not have access to water at all (SR=0), and 4 nodes can achieve SR values smaller than the ET (SR<0.7). Only 1 node has a SR=0.9.

Table 5. Case study 3. Nodal *SR* values in the no-valve scenario.

Node	SR no-valve	Node	SR no-valve
1	0.0	14	0.0
2	0.0	15	0.0
3	0.0	16	0.0
4	0.2	17	0.0
5	1.0	18	1.0
6	0.2	19	1.0
7	1.0	20	1.0
8	1.0	21	1.0
9	1.0	22	1.0
10	1.0	23	1.0
11	1.0	24	1.0
12	0.3	25	0.4
13	0.9		

Analysis of the simulation results also showed that, due the interposition of the tanks between nodes and users, some nodes upstream in the network overall receive an amount of water larger than the daily nodal water demand. In fact, such nodes continued receiving water volumes from the network until the water level in the tank remained below the value of H_{max} (even if the users have already received 100% of their demand). In this way, the flow is unable to move forward and to reach downstream parts of the network. Also, at the end of the day, upstream users had unused back-up water volume in their tanks. Conversely, other users (typically those far from the supply reservoir) received an amount of water smaller than the demand or, in the worst case, did not get any water at all.

Figure 13 shows the distribution of the flows in the network pipes at 2 a.m. at the condition of regime. The figure points out that only a portion of the 32 pipes conveys flows, while other pipes (those located far away from the reservoir, in the external loop of the network) remain (almost) empty for the whole duration of the simulation. This means that the presence of the tanks led a part of the network to be substantially disconnected from the supply reservoir. In detail, the figure highlights that in the no-valve scenario the flow mostly regards the district of the network immediately downstream the supply reservoir (node 27). In fact, nodes in this district (5, from 7 to 11 and from 18 to 22) have SR=1 (Table 5). Notably, the sum of the nodes daily average demand in such sub-network is about 30 l/s, that is very close to the value of the flow supplied to the whole distribution system. The flow is able to reach also nodes 23, 24 and 25 (even if with a minor intensity testified by the fact the pipes 22-23, 23-24 and 24-25 are not red coloured as the pipes the district immediately downstream the reservoir). Nodes in the north-east part of the network (from 1 to 4, 12 and from 14 to 17) are not reached by the flow or receive a minimum amount of water (Table 5).

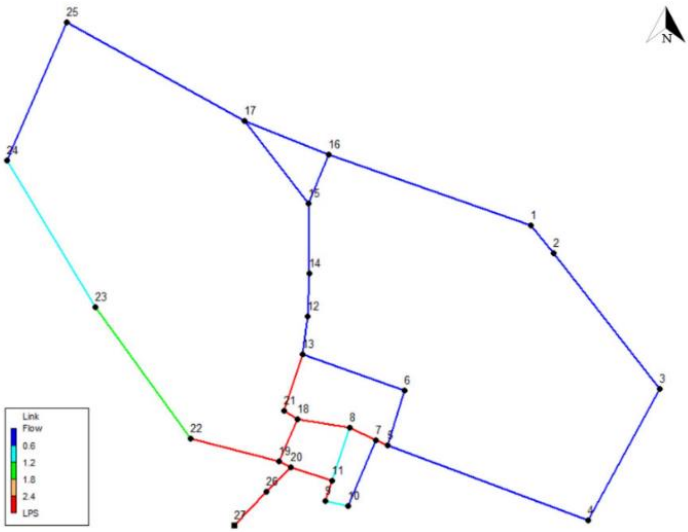

Figure 13. Case study 3. Distribution of the flow in the network pipes in the no-valve scenario at 2 a.m. of the 14th day of simulation.

Figure 14 shows that the equivalent tanks in the system significantly reduced the value at regime of *UC* from 1.0 down to 0.26 (achieved after about 7 days from the beginning of the water supply period). The general trend of the *UC* curve also reflects the influence of the initial conditions (empty pipes and tanks) in the simulation. As already discussed, the increasing values of the index are to be ascribed to the progressive achievement of the daily inflow/outflow balance. Preliminary simulations allowed establishing that a duration of 14 days is sufficient to assure the achievement of the conditions of regime for all the configurations explored in this work.

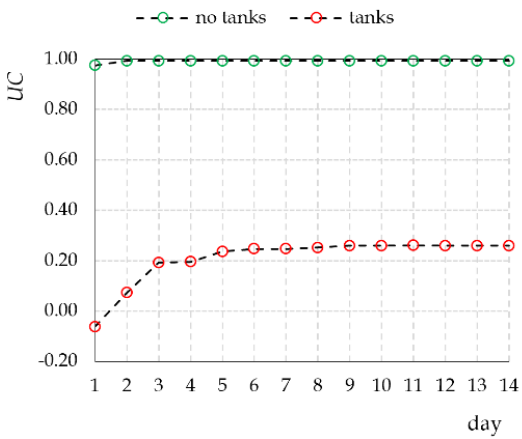

Figure 14. Case study 3. Simulation of the network in the no-valve scenario with and without private tanks. Value of *UC* as a function of the simulation time.

SA of gate valves

Application of the four steps of the SA algorithm described in sub-section 3.3.1. led to identify the optimal position of the first gate valve in the pipe between nodes 18 and 19, followed by the second gate valve in the pipe between nodes 8 and 11, and by the third one in the pipe between nodes 12 and 14, respectively. Simulations to evaluate further addition of gate valves in the network did not provide significant increase in the *UC* index. Figure 15 summarizes the results of the application of SA algorithm in terms of value of *UC* achieved at the condition of regime for every additional gate valve installed in the network. The figure shows the achievement of a significant increase in the equity of the water distribution as obtained

with the introduction of the first gate valve in the network with a value of *UC* at regime that achieves 0.66. Notably, the value of the index grows up to 0.75 and 0.78 in the configurations with 2 and 3 gate valves, respectively. Indeed, the added benefit of the sequential addition of the valves is always decreasing, with the addition of the fourth valve resulting in a negligible improvement of *UC*.

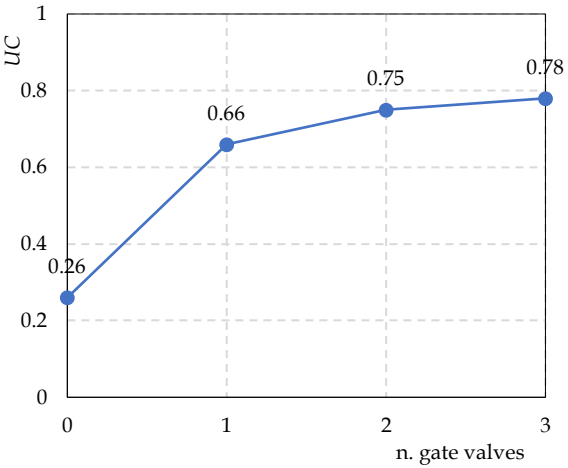

Figure 15. Case study 3. Results of SA of gate valves. Values of *UC* as a function of the number of gate valves.

Table 6 reports nodal *SR* values as obtained in the solution with 3 gate valves and the comparison with the corresponding values in the no-valve scenario. The re-arrangement of the water circulation in the network induced by the valves allows to increase the level of global equity among users. This is demonstrated by the increment of *UC* due to more uniform nodal *SR* values as compared to the no-valve scenario. Going into details of the single node, some of them (nodes

from 1 to 4, 6, from 14 to 17, and 25) increase their *SR*, while other nodes (nodes 5, from 7 to 11, from 18 to 20, from 22 to 24) are not impacted by the installation of the valves. The detailed analysis of the simulation results shows that the gate valves act as obstacles for the flow trying to feed the district immediately downstream the supply reservoir. In this way, the flow is forced to change its preferential paths, thus being able to reach disadvantaged nodes in the external loop of the network (this is the case of nodes from 1 to 4, 6, from 14 to 17, and 25 that did not receive water at all or received very small amount of water in the no-valve scenario). However, the re-distribution of the flows results in the decrease of *SR* down to 0.7 for two nodes (nodes 12 and 13 that reduce from 0.3 to 0 and from 0.9 to 0.1, respectively), thus potentially being cause of complaints by users supplied by that nodes (unless specific local supply countermeasures are not implemented). The fact that some nodes of the WDS could "pay" with unacceptable decreases in their SR to allow the increase in the global equity represents a limitation of the proposed SA algorithm of gate valves. In fact, such a behaviour could potentially be the cause of complaints by users supplied by those nodes, unless specific local supply countermeasures are not implemented together with valve installation. Remarkably, also node 21 shows *SR* to decrease, although the value of *SR* at regime is acceptable as it remains over the *ET* of 0.7.

Table 6. Case study 3. Nodal *SR* in the solutions with 3 gate valves and with 4 control valves provided by SA algorithms and comparison with the no-valve scenario.

Node	SR no-valve	SR 3 gate valves	SR 4 control valves	Node	SR no-valve	SR 3 gate valves	SR 4 control valves
1	0.0	1.0	0.3	14	0.0	1.0	1.0
2	0.0	1.0	0.0	15	0.0	1.0	1.0
3	0.0	1.0	0.0	16	0.0	1.0	1.0
4	0.2	0.8	0.2	17	0.0	1.0	1.0
5	1.0	1.0	0.8	18	1.0	1.0	1.0
6	0.2	0.5	0.2	19	1.0	1.0	1.0
7	1.0	1.0	1.0	20	1.0	1.0	1.0
8	1.0	1.0	1.0	21	1.0	0.7	1.0
9	1.0	1.0	1.0	22	1.0	1.0	1.0
10	1.0	1.0	1.0	23	1.0	1.0	1.0
11	1.0	1.0	1.0	24	1.0	1.0	1.0
12	0.3	0.0	0.6	25	0.4	1.0	1.0
13	0.9	0.1	0.8				

SA of control valves

Application of the six steps of the SA algorithm described in sub-section 3.3.1. provided the following optimal configuration with 4 control valves in the network: valve 1 (K=125) in the pipe between nodes 7 and 8, valve 2 (gate valve) in the pipe between nodes 6 and 13, valve 3 (K=2000) in the pipe between nodes 9 and 11, and valve 4 (K=60000) in the pipe between nodes 18 and 19. The introduction of a fifth valve did not provide further significant increment of the value

of *UC*. The value of the equity index achieved at regime under the final configuration with 4 control valves is 0.65. Figure 16 summarizes the results of the application of SA algorithm in terms of value of *UC* achieved at the condition of regime for every additional control valve installed in the network.

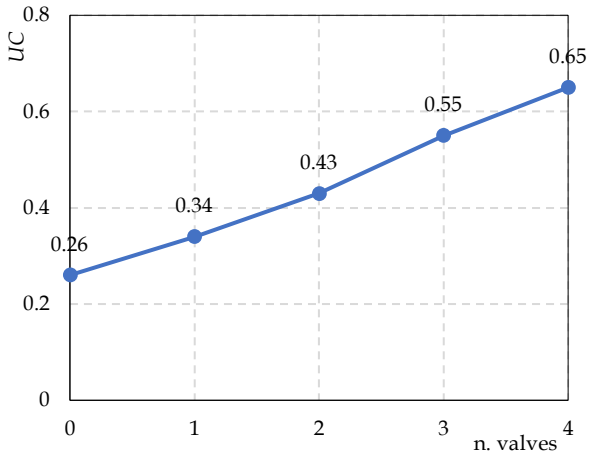

Figure 16. Case study 3. Results of SA of control valves. Values of *UC* as a function of the number of valves.

It should be stressed that the value of *UC* obtained with 4 valves using this second SA algorithm is lower than the value of UC obtained with 3 gate valves (Figure 15). However, local negative impacts due to the change of flow circulation as determined by the placement of the valves were shown to be mitigated by setting some of the valves as partially open. Table 6 reports nodal *SR* values at regime for the 25 demand nodes of the network as obtained with the 4 control valves

installed, and the comparison of these values with related *SR* values in the no-valve scenario. The results reveal nodes 1, 12, nodes 14-17, and node 25 to improve their *SR* value. Other nodes (nodes 2-4, 6-11, and 18-24) are not impacted by the installation of the valves. Finally, nodes 5 and 13 reduced their SR value (from 1.0 and 0.9 to 0.8, respectively), but they always remained over the *ET* of 0.7. Thanks to the additional nodal check of this second problem setting of SA algorithm, there are no decreasing of *SR* values under the *ET*.

NSGA II with gate valves

The first optimization scheme was applied using a population of 50 individuals and a total number of 100 generations. Since the case study is a 5-loops network with one source node (see Figure 11), a maximum of 5 gate valves was fixed in the optimization scheme. A larger number of valves would unavoidably result in the topological disconnection of network nodes from the source.

In Figure 17 the final Pareto front (reached after 50 generations) is shown. Values of UC in the Pareto front are referred to the condition of regime (i.e., 14th day of the simulation). In detail, the GA provided a solution with 1 gate valve located in the pipe between nodes 18-19 and a solution with 2 gate valves located in the pipes between nodes 5-6 and 13-21, respectively. Notably, there are not solutions with more than 2 gate valves. This means that the GA did not find solutions with 3 or more valves that perform better than the solution with 2 valves.

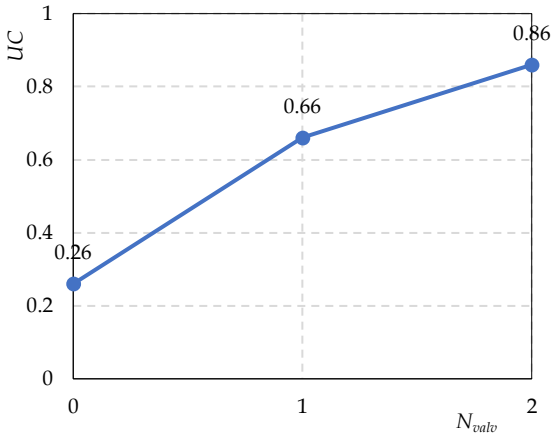

Figure 17. Case study 3. Results of the GA with gate valves. Values of UC as a function of N_{valv}.

The re-arrangement of the flow circulation as induced by the valves in the WDS allows increasing the level of global equity among users. This is demonstrated by the values of *UC* that grow from 0.26 (no-valve scenario) to 0.66 and 0.86 in the solutions with 1 and 2 gate valves, respectively. Table 7 reports nodal *SR* values at regime for all the demand nodes as obtained by the solution with 2 gate valves. Some nodes (from 1 to 4, 12, from 14 to 17, and 25) increase their SR as compared to the no-valve scenario, while other nodes (nodes 5, from 7 to 11, from 18 to 24) are not impacted by the installation of the valves. However, the re-distribution of the flows results in the worsening of conditions for two nodes of the WDS (nodes 6 and 13). In particular, node 6 - that starts with a *SR* value (0.2) already lower than *ET* - now provides *SR*=0. Also, *SR* for node 13 reduces from 0.9 to 0.3, thus

dropping down below the *ET*. As before for SA algorithm of gate valves, these unfair decreasing in nodal *SR* represent a limitation of the first NSGA II-based optimization scheme.

Table 7. Case study 3. Nodal *SR* in the solutions with 2 gate valves and with 4 control valves provided by NSGA II algorithms and comparison with the no-valve scenario.

Node	SR no-valve	SR 2 gate valves	SR 4 control valves	Node	SR no-valve	SR 2 gate valves	SR 4 control valves
1	0.0	1.0	0.2	14	0.0	1.0	0.9
2	0.0	1.0	0.0	15	0.0	1.0	0.9
3	0.0	1.0	0.0	16	0.0	1.0	1.0
4	0.2	1.0	0.2	17	0.0	1.0	1.0
5	1.0	1.0	1.0	18	1.0	1.0	1.0
6	0.2	0.0	0.2	19	1.0	1.0	1.0
7	1.0	1.0	1.0	20	1.0	1.0	1.0
8	1.0	1.0	1.0	21	1.0	1.0	1.0
9	1.0	1.0	1.0	22	1.0	1.0	1.0
10	1.0	1.0	1.0	23	1.0	1.0	1.0
11	1.0	1.0	1.0	24	1.0	1.0	1.0
12	0.3	0.9	0.3	25	0.4	1.0	1.0
13	0.9	0.3	0.7				

Figure 18 shows the flow distribution in the WDS for the solution with 2 valves. When two gate valves are positioned between nodes 5-6 and 13-21 respectively, the flow is forced to change the preferential paths followed in the no-valve scenario (Figure 13). Pipes 5-6 and 13-21 are located in the district just downstream of the supply reservoir.

Therefore, these gate valves are able to limit the flow towards the network district immediately downstream of the reservoir. Figure 16 shows a significant deviation of the flow coming from the supply reservoir (node 27) toward the external loop of the network. This new distribution of the flow inside the network explains the increase in *SR* for nodes 1 to 4, 12, 14 to 17 and 25 as compared to the no-valve scenario (Table 7). On the other hand, the position of the valves between nodes 5-6 and 13-21 is most likely the cause of the worsening of the *SR* for nodes 6 and 13 (these nodes are immediately downstream the gate valves).

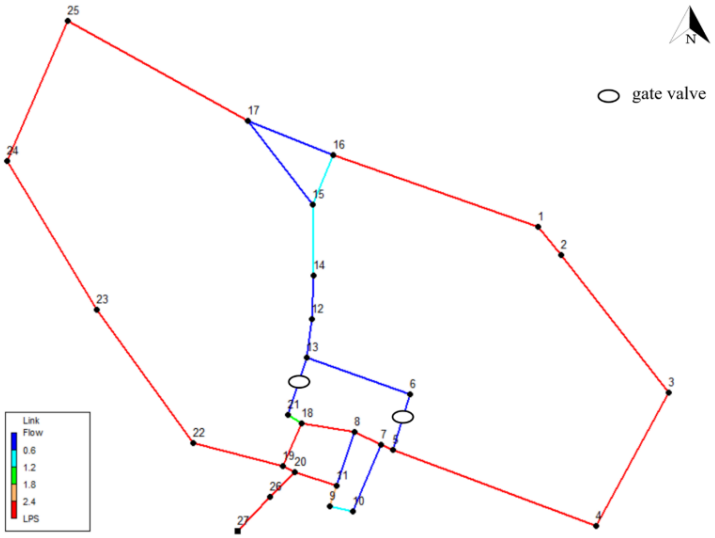

Figure 18. Case study 3. Distribution of the flow in the network pipes in the solution with 2 gate valves installed at 2 a.m. of the 14th day of simulation.

The GA reached the 50th generation in almost 15 days. Computational time involved in the optimization processes is currently the weakest point of the methodology and deserves further discussion. Times of computations with a standard PC are still rather high, thus allowing use of the methodology only as offline application for objectives of network design or rehabilitation. A general remark is that large part of the computational effort is related to the evaluation of the first objective function (which involves cross-simulation of the network with EPA-SWMM). This means that time of computation can be reduced significantly if simplifications are performed in modelling the network with EPA-SWMM.

NSGA II with control valves

The second optimization scheme was applied with a population of 70 individuals and a total number of 200 generations. The increased population and generations as compared to the first scheme follow the increased complexity of the algorithm due to the wider research-space of the GA because valves can take different degrees of closure. In order to reduce the computational time, a maximum number of 4 control valves was considered. Moreover, differently from SA of control valves, the settings of partially open valves have to be chosen in advance. A set of 3 *K*-values (50, 1500 and 20000) was given as input to the GA for the valves setting. The selected *K*-values may correspond to different valve settings according to the type of valve chosen for the installation. A brief analysis of the relationships between *K* and the

valve closure degree for several types of valves available in the market pointed out that the chosen *K* values correspond to degrees of closure between 84 and 99%. This range of degree of closure has proven to be effective in obtaining good results in the previous applications with SA algorithms.

In Figure 19 the final Pareto front (reached after 30 generations) is shown. The GA provided solutions with up to 4 control valves. In detail, the solution with 1 control valve (K=50) in the pipe between nodes 5-6 does not lead to a significant increase of *UC*. The solution with 2 control valves in the pipes between nodes 5-7 and 18-19 (*K*=50 and *K*=20000, respectively) allows reaching a UC value of 0.59. Solutions with 3 and 4 control valves provide almost the same *UC* value (0.60) with following configurations: 3 valves between nodes 5-7, 15-17 and 18-19 (*K*=50, gate valve and *K*=20000, respectively), and 4 valves between nodes 5-7, 5-6, 15-17 and 18-19 (*K*=50 the first two and *K*=20000 the last two). Even in this case, solutions provided by the algorithm include valve positions in network pipes belonging to the district immediately downstream of the reservoir. Notably, the maximum *UC* provided by this optimization scheme is considerably lower than the UC value obtained with use of the first scheme. On the other hand, no node worsens unacceptably its condition as compared to the no-valve scenario. Table 7 reports the nodal SR values for the 25 demand nodes of the network as obtained with the 4 valves installed. In the configuration with 4 control valves, some nodes (1, from 14 to 17 and 25) increase their *SR* as compared to the no-valve scenario,

while other nodes (from 2 to 12 and from 18 to 24) are not impacted by the installation of the valves. There is also a node (13) that worsens its condition as compared to the no-valve scenario. However, this worsening would be "allowed" since node 13 starts with a *SR*>*ET* and does not drop its *SR* value under the threshold.

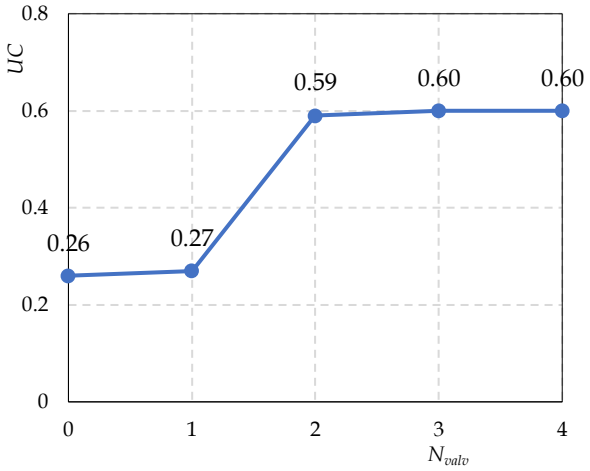

Figure 19. Results of the GA with control valves. Values of *UC* as a function of N_{valv}.

It should be stressed that both methodologies for optimal location of valves (SA and NSGA II algorithms) does not assure the improvement of the nodal *SR* value for all the network nodes, since they do not involve local interventions at the level of the single node. However, applying the second optimization schemes for control valves, water service providers may assure that no node worsens

unacceptably its condition as compared to the current scenario with no valves installed.

Due to the increased complexity of the GA, the convergence of the simulation was reached after about 55 days of simulation.

Simulations were also run by limiting the set of locations for the control valves in the WDS. Application of the procedure described early in the methodological chapter of the paper, allowed reducing to 20 out of 32 pipes the valve locations (pipes from 5 to 14, 16 and 17, from 22 to 28 and 32, see Table ST5). The final Pareto front (Figure 20) was reached after 18 generations. The figure shows that the GA provided solutions up to 3 control valves. The solution with 1 control valve is, in practice, the same as that obtained in the previous running of the GA. Solutions with 2 and 3 control valves provide almost the same UC value (0.59) and have the following configurations: 2 valves between nodes 7-8 and 18-19 (K=1500 and K=20000, respectively), and 3 valves between nodes 7-8, 18-21 and 18-19 (K=1500, K=50 and K=20000, respectively). Moreover, there is not a solution with 4 control valves in the Pareto front shown in Figure 20. This can be ascribed to the reduced number of pipes in which the valves can be installed in this additional application of the second optimization scheme. As an example, one of the valves in the solution with 4 valves in Figure 19 is located in a pipe (between node 15 and 17), which is not allowed to have a valve installed in the run of the GA with restriction of the research space.

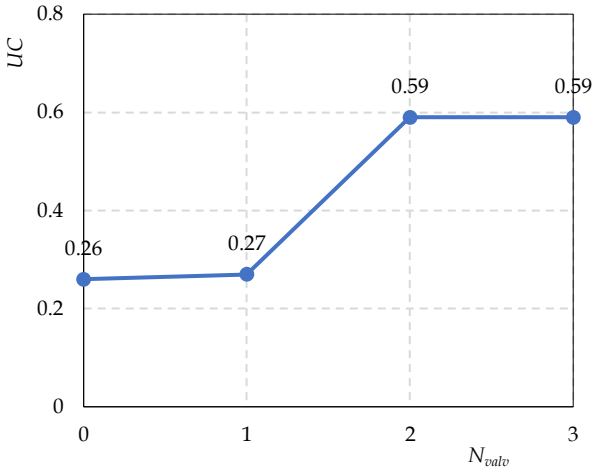

Figure 20. Case study 3. Results of the GA with control valves and restrictions on valve positioning. Values of UC as a function of N_{valv}.

With the restriction in valves positioning, the GA converged in less than 25 days, thus significantly faster than before. As told before, the GA in the second scheme involves a larger computational effort since, beside the optimization of valve locations, it is also required to optimize the valves setting. However, through reasonable reduction of the research space (limitation of the possible valve locations), the GA may be able to reach the convergence in a smaller number of generations (18 instead of 30) with a total time saving of over 50%.

Comparison of the two methodologies for optimal location of control valves

Results presented in previous paragraphs show that both SA algorithms and NSGA II are valid methodologies for identifying optimal locations of control valves to improve equity in water

distribution among users. However, the comparison of the two methodologies deserves further discussion.

A general consideration is that the application of the proposed GA involves a computational effort much higher than SA algorithms. On the other hand, the GA performs a better exploration of the research space as compared to SA algorithms. The last ones indeed, allows to find only a local optimum due to the limitation of the methodologies itself. The comparison of the results obtained with the two methodologies for the first optimization scheme (only gate valves) allows to clarify this concept. Figures 15 and 17 point out that the GA performs better than SA algorithm in the first optimization scheme. In fact, the GA allows to obtain a value of *UC*=0.86 with only 2 gate valves. With the same number of gate valves, *UC* is equal to 0.75 in case of application of SA algorithm. Although the difference in values of *UC* is not so significant, a more in deep analysis of the solutions can highlight the difference between the two methodologies. Both GA and SA algorithm provide the same solution with 1 gate valves (in pipe between nodes 18-19). The application of the second step of SA algorithm allows to locate the second gate valve only in presence of the first gate valve already positioned. The position of the gate valves of previous steps represents a sort of boundary condition in this case. Therefore, the best the SA algorithm can find with the first valve already positioned is a solution with 2 gate valves that provide a *UC*=0.75. Instead, the GA can search for any couple of gate valves

and provide a solution with 2 gate valves that allows to reach a higher value of the equity coefficient as compared to SA algorithm.

Comparison of the performances of the 2 algorithms for the second optimization scheme (control valves with different closure settings) points out that the GA performs slightly better than SA algorithm for the solution with 3 valves, but the behaviour of the two algorithms is opposite for the solution with 4 valves (Figures 16 and 19). Indeed, it should be underlined that a great limitation of the GA in this second optimization scheme consists in the need to fix a priori a set of K-values for the valves setting. Therefore, in this case, the advantageous of a big research space of the GA are balanced (and potentially overcome) by the minor degree of freedom in the choice of K-values. At the end, for the case study analysed, the greater computational effort of the GA is not justified by better results as compared to those provided by SA algorithms.

Finally, a future development of the proposed methodologies could consider the use of turbines for energy recovery instead of control valves, in the wake of successful applications showed in the technical literature on the topic (De Marchis *et al.*, 2011; Carravetta *et al.*, 2014; Sinagra *et al.*, 2017). In this way, an initial greater financial effort would be justified by a potential return on investment. Moreover, after the pay-back period, the installation of such devices would allow long term benefits in terms of energy cost savings.

5. Conclusions

The present thesis reports the results of a research work carried out during a 3-years PhD course. The research regards intermittent WDSs. This term refers to a particular managing of water distribution systems increasingly adopted both in developing and developed countries around the world. Causes of intermittency in water supply are several and interconnected, involving environmental constraints (water shortage), technician deficiencies and economic issues. Under intermittent condition water companies can supply water for period less than 24 hours a day and/or less than 7 days a week. Otherwise, they can supply water continuously for 24 hours a day but making only a fraction of the network daily water demand available. In both cases, the behaviour of the system cannot be assimilated to traditional WDSs. As explained in the introduction chapter, these systems are characterized by low pressure throughout the network, cyclic phases of network filling/emptying with pipe alternatively switching from free surface to pressurized flow, water quality issues and last but not least, inequity in distribution of water resource among users. The unreliability of intermittent WDSs leads network users to install private storage facilities (basement or roof tanks) in their properties, in order to collect water as much as possible during the supply period. The presence of private tanks exacerbates problems of inequity among the network users in a sort of complex negative feedback loop. The background chapter highlighted the gap in knowledge of intermittent WDSs. Experimental data are rather scarce and proper software/tools

for the modelling of such systems have not been consolidated, yet. Strategies to improve equity in intermittent WDSs already proposed in literature often involve a large capital cost or can be applied only in early stage of the systems design (they are not managing strategies). The present work made a step forward in the analysis of intermittent WDSs both from experimental and modelling side. In the wake of first attempts by some authors, EPA-SWMM software – developed by the United States Environmental Protection Agency (US-EPA) - was individuated as potential tool for the modelling of intermittent WDSs. In fact, although the software was originally developed for the analysis of urban drainage systems, its capability to simulate both free-surface and pressurized flow makes it suitable for the analysis of intermittent WDSs. Moreover, the use of EPA-SWMM could allow for a widespread sharing of the results as well as a fast developing of the research because of its availability (free and open source software) and its great diffusion among both research institutes and business companies. Therefore, in a preliminary phase of the work settings and tools of EPA-SWMM software were adapted in a novel way to simulate elements and ways of operation of intermittent WDS. Then, the issue of equity in water distribution among users was investigated with the aim to propose a relatively simple and cheap managing strategy for the improvement of equity in existing intermittent WDSs. The strategy consists in placing control valves in strategic pipes of the network in order to change the flow circulation thus allowing for a better allocation of the water resource among users. Two different

optimization algorithms were set-up to achieve the objective underlying this strategy. A first simple one-objective optimization algorithm based on sequential addition (SA) of valves and a second multi-objectives optimization genetic algorithm based on the Non-Dominated Sorted Genetic Algorithm II (NSGA II). Three case study were individuated to apply and test the proposed methodologies/tools. The first case study was used to test the ability of EPA-SWMM to correctly reproduce the filling phase of a WDS. In fact, measurements about the filling process of the network of case study 1 were available from the field. The comparison between simulated and experimental data pointed out the suitability of EPA-SWMM to reproduce the network filling phase of the case study network. The second case study is a real intermittent WDS located in Sicily (Italy) and was monitoring during the years 2019-2020 thus allowing the collection of a wide experimental dataset. The network of case study 2 was also simulated with EPA-SWMM that showed to be able to manage all phases of an intermittent of a complex WDS with users equipped with private tanks. The network filling phase as simulated by EPA-SWMM was also compared to results provided by the application of a model based on the Rigid Water Column (RWC) theory – traditionally used in literature for the simulation of the network filling process. For this purpose, a simple and very flat network was selected (case study 3), thus assuring the basic hypothesis of the RWC model to be verified. As expected, the two models provided very similar results for the part of the network closer

to the supply reservoir. For the part of the network far from the reservoir, the results provided by the two models are slightly different, probably because of the occurring of free-surface flow that the RWC model is not able to manage. Finally, the third case study was also used for the application of the optimization algorithms aimed at finding optimal location and/or settings of control valves to improve equity in intermittent WDSs. The results of the application showed that both algorithms allow to increase the level of equity with the installation of few valves in specific network pipes. Limits and advantages of the two algorithms were also highlighted in the discussion of the results.

Globally, the results obtained in the different steps of the research project are satisfactory and open perspective for an improved use of EPA-SWMM for the analysis of intermittent WDSs. The proposed methodologies for optimal locations of valves showed how it is possible to obtain sensible increases in global equity among users installing few valves in the network pipes.

Supplementary material

Table ST1. Case study 1. Nodal elevation and average yearly demand.

Node	*z* (m a.s.l.)	yearly demand (l/s)	Node	*z* (m a.s.l.)	yearly demand (l/s)
1	712.00	0.12	29	727.00	0.00
2	707.51	0.36	30	719.00	0.12
3	702.18	0.78	31	711.08	0.06
4	687.00	0.00	32	705.00	0.12
5	686.26	0.54	33	700.36	0.30
6	687.00	0.00	34	757.00	0.36
7	666.00	0.00	35	749.00	0.36
8	650.00	0.00	36	746.24	0.60
9	660.70	0.06	37	746.00	0.06
10	671.00	0.48	38	751.08	0.30
11	671.43	0.06	39	758.02	0.06
12	670.35	0.00	40	760.00	0.06
13	670.35	0.22	41	738.75	1.02
14	674.10	0.00	42	735.83	0.36
15	710.39	2.16	43	719.99	0.18
16	711.04	0.00	44	717.36	1.92
17	723.25	0.06	45	717.36	0.48
18	711.50	0.06	46	715.00	0.00
19	731.53	0.00	47	713.02	0.00
20	728.19	0.06	48	712.00	0.00
21	757.02	0.18	49	719.80	0.42
22	741.38	0.06	50	720.20	0.24
23	777.19	0.00	51	722.67	0.00
24	772.00	0.00	52	716.52	0.06
25	772.00	0.02	53	725.00	0.00
26	762.00	0.06	54	725.00	0.06
27	737.13	0.72	55	745.72	0.00
28	727.21	0.18	56	764.60	0.00

Table ST2. Case study 1. Network pipe characteristics.

Pipe	Up node	Down node	L (m)	D (m)	k ($m^{1/3}/s$)
1	1	2	62.4	0.125	140
2	2	3	31.4	0.1	70
3	3	4	66.8	0.1	70
4	4	5	106.2	0.1	70
5	5	6	152.7	0.1	70
6	6	7	186.7	0.1	70
7	7	8	209.7	0.1	70
8	8	9	177.9	0.1	70
9	9	10	133.7	0.1	70
10	10	11	177	0.05	85
11	11	12	172.39	0.025	85
12	12	13	100	0.025	85
13	12	14	88.03	0.025	85
14	10	15	380.3	0.1	70
15	15	16	51.1	0.06	140
16	16	17	91.78	0.06	140
17	16	18	50	0.06	140
18	15	19	167.8	0.1	70
19	19	20	134.2	0.1	70
20	19	21	177.1	0.1	70
21	21	22	281.2	0.06	70
22	21	23	183.1	0.2	70
23	23	24	383.9	0.15	70
24	24	25	69.9	0.1	70
25	25	26	161.7	0.1	70
26	26	27	132.4	0.1	70
27	27	28	167.3	0.1	70
28	28	29	34.5	0.1	70
29	29	30	69.2	0.1	70
30	30	31	121.3	0.1	70
31	31	32	47.6	0.1	70
32	32	33	93.9	0.1	70
33	33	9	345.1	0.16	140
34	26	34	73	0.1	70
35	34	35	98.3	0.1	70

Table ST2 (continued). Case study 1. Network pipe characteristics.

Pipe	Up node	Down node	L (m)	D (m)	k ($m^{1/3}/s$)
36	35	36	94.8	0.15	70
37	36	37	80.1	0.032	85
38	37	38	58.5	0.1	70
39	38	39	41.4	0.1	70
40	39	40	117.8	0.1	70
41	38	34	184.8	0.032	85
42	36	41	67.1	0.15	70
43	41	42	110.3	0.125	70
44	42	43	242.3	0.125	70
45	43	44	51.5	0.125	70
46	44	45	13.7	0.125	70
47	45	46	72.6	0.125	85
48	46	47	43.2	0.125	85
49	47	48	48.6	0.125	85
50	48	2	102.5	0.125	85
51	44	49	60	0.08	85
52	49	50	75.6	0.08	70
53	50	51	62.3	0.1	70
54	51	52	95.1	0.05	85
55	51	53	184.6	0.1	70
56	53	54	20.6	0.1	70
57	53	55	179.1	0.1	70
58	55	56	364.4	0.1	85

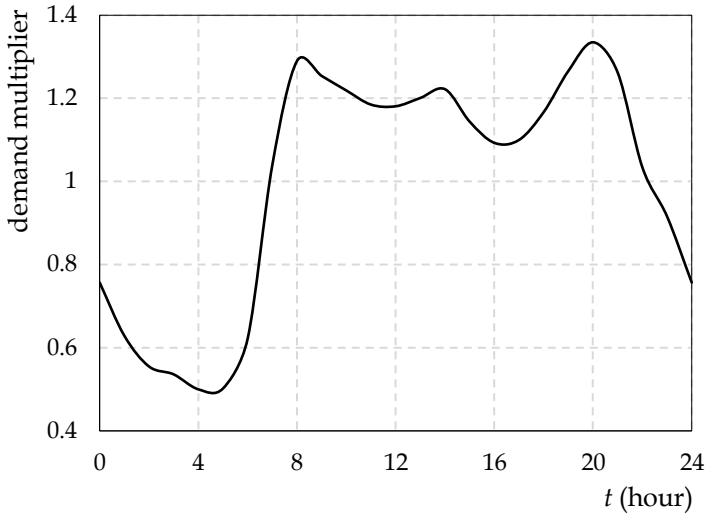

Figure SF1. Case studies 2-3. Daily pattern of the nodal water demands in the network.

Table ST4. Case study 3. Nodal average daily demands.

Node	daily demand (l/s)
1	1.38
2	0.18
3	0.92
4	2.57
5	2.83
6	8.36
7	3.42
8	5.33
9	1.52
10	0.86
11	2.27
12	1.31
13	8.52
14	0.88
15	0.22
16	0.39
17	0.45
18	2.82
19	0.03
20	0.31
21	2.60
22	1.03
23	1.00
24	0.53
25	0.76
26	0.00
27	0.00

Table ST5. Case study 3. Network pipe characteristics.

Pipe	Up node	Down node	*L* (m)	*D* (mm)	Roughness (Manning coeff.) (s/m$^{1/3}$)
1	1	2	10.1	100	0.01
2	2	3	2874.5	125	0.01
3	3	4	1732.8	150	0.01
4	1	16	2851.4	125	0.01
5	4	5	2648	200	0.01
6	5	7	144.5	200	0.01
7	5	6	364.9	200	0.01
8	7	10	817.4	150	0.01
9	6	13	1269.8	200	0.01
10	7	8	332.7	300	0.01
11	8	11	628.3	150	0.01
12	9	10	269.7	150	0.01
13	11	9	241.3	150	0.01
14	8	18	887.8	300	0.01
15	12	14	2055.9	150	0.01
16	13	12	130.9	250	0.01
17	21	13	991.1	250	0.01
18	14	15	6.8	200	0.01
19	15	16	607.2	150	0.01
20	15	17	1669.7	125	0.01
21	17	16	1046.8	150	0.01
22	18	21	132.1	300	0.01
23	18	19	392.5	450	0.01
24	19	20	154.5	450	0.01
25	22	23	2469.3	200	0.01
26	22	19	1593.6	250	0.01
27	24	23	2567	125	0.01
28	25	24	2337.7	100	0.01
29	17	25	2452.7	150	0.01
30	27	26	19.6	450	0.01
31	26	20	9.6	450	0.01
32	20	11	490.9	150	0.01

References

Al-Ghamdi, A. S. (2011). "Leakage-pressure relationship and leakage detection in intermittent water distribution systems." J. Water Supply: Res. Technol.- Aqua, 60(3), 178–183.

Alvisi S., & Franchini M. (2009). "Multiobjective Optimization of Rehabilitation and Leakage Detection Scheduling in Water Distribution Systems". Journal of Water Resource Planning and Management, 135(6), 426-439. https://doi.org/10.1061/(ASCE)0733-9496(2009)135:6(426)

Ameyaw, E. E., Memon, F. A., & Bicik, J. (2013). Improving equity in intermittent water supply systems. Journal of Water Supply: Research and Technology - AQUA, 62(8), 552–562. https://doi.org/10.2166/aqua.2013.065

Arregui, F., Cabrera, E. Jr., & Cobacho, R. (2007). Integrated Water Meter Management. IWA Publishing, London.

Braun, M., Piller, O., Deuerlein, J., Mortazavi, I., & Gmbh, C. (2017). Limitations of demand- and pressure-driven modeling for large deficient networks, (1963), 93–98.

Cabrera-Bejar, J. A., & Tzatchkov, V. G. (2009). Inexpensive Modeling of Intermittent Service Water Distribution Networks. World Environmental and Water Resources Congress 2009, 295–304. https://doi.org/10.1061/41036(342)29

Campisano, A., Ph, D., & Modica, C. (2016). Two-Step Numerical Method for Improved Calculation of Water Leakage by Water Distribution Network Solvers. 1–11. https://doi.org/10.1061/(ASCE)WR.1943-5452.0000598.

Carravetta, A., Fecarotta, O., Sinagra, M. & Tucciarelli, T. (2014). Cost-Benefit Analysis for Hydropower Production in Water Distribution Networks by a Pump as Turbine. J. Water Resour. Plann. Manag. 2014, 140, 04014002.

Ciaponi, C., & Creaco, E. (2018). Comparison of pressure-driven formulations for WDN simulation. Water (Switzerland), 10(4). https://doi.org/10.3390/w10040523

Cobacho, R., Arregui, F., Cabrera, E., & Cabrera, E. Jr. (2008). Private water storage tanks: evaluating their inefficiencies. Wat. Prac. Technol. 3(1).

Commission of the European Communities. (2007). Addressing the Challenge of Water Scarcity and Droughts in the European Union: Impact Assessment. Brussels: SEC(2007) 993.

Creaco, E., & Pezzinga, G. (2018). Comparison of algorithms for the optimal location of control valves for leakage reduction in WDNs. Water (Switzerland), 10(4), 1–13. https://doi.org/10.3390/w10040466

Creaco, E., & Walski, T. (2017). Economic Analysis of Pressure Control for Leakage and Pipe Burst Reduction. Journal of Water

Resources Planning and Management, 143(12), 04017074. https://doi.org/10.1061/(ASCE)WR.1943-5452.0000846

Creaco, E., Franchini, M., & Alvisi, S. (2010). "Optimal Placement of Isolation Valves in Water Distribution Systems Based on Valve Cost and Weighted Average Demand Shortfall." Water Resources Management, 24(15), 4317–4338. https://doi.org/10.1007/s11269-010-9661-5

Creaco, E., Franchini, M., & Todini, E. (2016). "The combined use of resilience and loop diameter uniformity as a good indirect measure of network reliability." Urban Water Journal, 13(2), 167–181. https://doi.org/10.1080/1573062X.2014.949799

Criminisi, A., Fontanazza, C. M., Freni, G., & La Loggia, G. (2009). Evaluation of the apparent losses caused by water meter under-registration in intermittent water supply. Water Science and Technology, 60(9), 2373–2382. https://doi.org/10.2166/wst.2009.423

Darcy, H. (1857). Recherches expérimentales relatives au mouvement de l'eau dans les tuyaux. Mallet-Bachelier, Paris. 268 pages and atlas (in French).

De Marchis, M., Fontanazza, C. M., Freni, G., La Loggia, G., Napoli, E., & Notaro, V. (2011). Analysis of the impact of intermittent distribution by modelling the network-filling process. Journal of

Hydroinformatics, 13(3), 358. https://doi.org/10.2166/hydro.2010.026

De Marchis, M., Fontanazza, C. M., Freni, G., La Loggia, G., Napoli, E., & Notaro, V. (2010). A model of the filling process of an intermittent distribution network. Urban Water Journal, 7(6). https://doi.org/10.1080/1573062X.2010.519776

De Marchis, M., Fontanazza, C. M., Freni, G., Milici, B., & Puleo, V. (2014). Experimental investigation for local tank inflow model. Procedia Engineering, 89, 656–663. https://doi.org/10.1016/j.proeng.2014.11.491

De Marchis, M., Fontanazza, C., Freni, G., La Loggia, G., Napoli, E. & Notaro, V. (2011). Analysis of the impact of intermittent distribution by modelling the network-filling process. J. Hydroinf. 2011, 13, 358–373.

De Marchis, M., Milici, B., & Freni, G. (2015). Pressure-discharge law of local tanks connected to a water distribution network: Experimental and mathematical results. Water (Switzerland), 7(9), 4701–4723. https://doi.org/10.3390/w7094701

European Commission. (2012). Report on the Review of the European Water Scarcity and Droughts Policy. Brussels: COM (2012) 672 final.

Farina G., Creaco E., & Franchini M. (2014). Using EPANET for modelling water distribution systems with users along the pipes. Civil Engineering and Environmental Systems, 31(1), 36-50.

Farley, M., & Trow, S. (2003). Losses in water distribution networks: A practitioner's guide to assessment, monitoring and control. IWA Publishing, London.

Farmani R., Walters G., & Savic D. (2006). "Evolutionary multi-objective optimization of the design and operation of water distribution network: total cost vs. reliability vs. water quality." Journal of Hydroinformatics, 8(3), 165-179. https://doi.org/10.2166/hydro.2006.019b

Ferrante, M. (2012). "Experimental investigation on the effects of pipe material on the leak head discharge relationship." J. Hydraul. Eng., 10.1061/(ASCE)HY.1943-7900.0000578, 736–743.

Fontanazza, C. M., Freni, G., & La Loggia, G. (2007). Analysis of intermittent supply systems in water scarcity conditions and evaluation of the resource distribution equity indices. WIT Transactions on Ecology and the Environment, 103, 635–644. https://doi.org/10.2495/WRM070591

Galaitsi, S. E., Russell, R., Bishara, A., Durant, J. L., Bogle, J., & Huber-Lee, A. (2016). Intermittent domestic water supply: A critical review and analysis of causal-consequential pathways. Water (Switzerland), 8(7). https://doi.org/10.3390/w8070274

Gottipati, P. V. K. S. V., & Nanduri, U. V. (2014). Equity in water supply in intermittent water distribution networks. Water and Environment Journal, 28(4), 509–515. https://doi.org/10.1111/wej.12065

Guizani M., Vasconcelos J. G., Wright S. J. & Maalel K. (2005). Invetigation of rapid filling of empty pipes. Intelligent Modeling of Urban Water Systems, Monograph 14. W. James, K. N. Irvine, E. A. McBean & R.E. Pitt, Eds. ISBN 978-0-9736716-2-9 © CHI 2006

Ilaya-Ayza, A. E., Benítez, J., Izquierdo, J., & Pérez-García, R. (2017a). Multi-criteria optimization of supply schedules in intermittent water supply systems. Journal of Computational and Applied Mathematics, 309, 695-703

Ilaya-Ayza, A. E., Martins, C., Campbell, E., & Izquierdo, J. (2017b). Implementation of DMAs in intermittent water supply networks based on equity criteria. Water, 9(11), 851

Klingel, P. (2012). Technical causes and impacts of intermittent water distribution. Water Science and Technology: Water Supply, 12(4), 504–512. https://doi.org/10.2166/ws.2012.023

Kumpel E. & Nelson K. L. (2015). Intermittent Water Supply: Prevalence, Practice, and Microbial Water Quality. Environmental Science & Technology 2016 50 (2), 542-553. ACS Publications. https://doi.org/10.1021/acs.est.5b03973

Liou, C. P. & Hunt, W. A. (1996). Filling of pipelines with undulating elevation profiles. J. Hydr. Engrg., 122(10), 534-539.

Manish, S., & Buchberger, S. G. (2012). Role of Satellite Water Tanks in Intermittent Water Supply System Manish. Environmental, World Program, Environmental Engineering, (Yepes 2001), 944–951. https://doi.org/doi:10.1061/9780784412312.096

Mays, L. W. (1999). Water distribution systems handbook. McGraw Hill Professional.

Milano V. (2012). Acquedotti – Guida alla progettazione. Second edition. Hoepli Editor. Milano (Italy)

Mokssit, A., de Gouvello, B., Chazerain, A., Figuères, F., & Tassin, B. (2018). Building a Methodology for Assessing Service Quality under Intermittent Domestic Water Supply. Water 2018, Vol. 10, Page 1164, 10(9), 1164. https://doi.org/10.3390/W10091164

Molden, D. J. & Gates, T. K. (1990) Performance measures for evaluation of irrigation water delivery systems. Journal of Irrigation and Drainage Engineering 116, 804–823.

Pezzinga, G., & Gueli, R. (1999). Discussion of Optimal Location of Control Valves in Pipe Networks by Genetic Algorithm. J. Water Resour. Plan. Manag. 125, 65–67

Rossman, L. A. (2000). EPANET 2 Users Manual. United States Environment Protection Agency.

Rossman, L. A. (2015). Storm Water Management Model User's Manual Version 5.1. United States Environment Protection Agency.

Simukonda, K., Farmani, R., & Butler, D. (2018). Intermittent water supply systems: causal factors, problems and solution options. Urban Water Journal, 15(5), 488–500. https://doi.org/10.1080/1573062X.2018.1483522

Sinagra, M., Sammartano, V., Morreale, G. & Tucciarelli, T. (2017). A New Device for Pressure Control and Energy Recovery in Water Distribution Networks. Water. 9. 309. 10.3390/w9050309.

Soltanjalili, M. J., Bozorg Haddad, O., & Mariño, M. A. (2013). Operating water distribution networks during water shortage conditions using hedging and intermittent water supply concepts. Journal of Water Resources Planning and Management, 139(6), 644-659

Wagner, J. M., Shamir, U. & Marks, D. H. (1988). Water distribution reliability: simulation methods. J. Wat. Res. Plann. Manage. 114(3), 276–294

Wang, Q., Wang, L., Huang, W., Wang, Z., Liu, S., & Savić, D. A. (2019). Parameterization of NSGA-II for the optimal design of water distribution systems. Water (Switzerland), 11(5). https://doi.org/10.3390/w11050971